AD-A033 536 MISSION RESEARCH CORP SANTA BARBARA CALIF F/G 20/3
ANALYTIC SGEMP ANALYSIS FOR A PERFECTLY CONDUCTING SPHERE.(U)
MAY 76 R STETTNER DNA001-76-C-0086
UNCLASSIFIED MRC-R-269 DNA-4033T

1 OF 1
ADA
033536

END
DATE
FILMED
1-25-77
NTIS

ANALYTIC SGEMP ANALYSIS FOR A PERFECTLY CONDUCTING SPHERE

Mission Research Corporation,
Santa Barbara, California

May 1976

DNA 4033T

ANALYTIC SGEMP ANALYSIS FOR A PERFECTLY CONDUCTING SPHERE

Mission Research Corporation
735 State Street
Santa Barbara, California 93101

May 1976

Topical Report

CONTRACT No. DNA 001-76-C-0086

THIS WORK SPONSORED BY THE DEFENSE NUCLEAR AGENCY
UNDER RDT&E RMSS CODE B323076464 R99QAXEB06964 H2590D.

Prepared for
Director
DEFENSE NUCLEAR AGENCY
Washington, D. C. 20305

DESTROY THIS REPORT WHEN IT IS NO LONGER NEEDED. DO NOT RETURN TO SENDER.

UNCLASSIFIED

SECURITY CLASSIFICATION OF THIS PAGE *(When Data Entered)*

REPORT DOCUMENTATION PAGE		READ INSTRUCTIONS BEFORE COMPLETING FORM
1. REPORT NUMBER DNA 4033T	2. GOVT ACCESSION NO.	3. RECIPIENT'S CATALOG NUMBER
4. TITLE *(and Subtitle)* ANALYTIC SGEMP ANALYSIS FOR A PERFECTLY CONDUCTING SPHERE		5. TYPE OF REPORT & PERIOD COVERED Topical Report 6. PERFORMING ORG. REPORT NUMBER MRC-R-269
7. AUTHOR(s) Roger Stettner		8. CONTRACT OR GRANT NUMBER(s) DNA 001-76-C-0086
9. PERFORMING ORGANIZATION NAME AND ADDRESS Mission Research Corporation 735 State Street Santa Barbara, California 93101		10. PROGRAM ELEMENT, PROJECT, TASK AREA & WORK UNIT NUMBERS R99QAXEB069-64
11. CONTROLLING OFFICE NAME AND ADDRESS Director Defense Nuclear Agency Washington, D.C. 20305		12. REPORT DATE May 1976 13. NUMBER OF PAGES ~~80~~ 72
14. MONITORING AGENCY NAME & ADDRESS*(if different from Controlling Office)*		15. SECURITY CLASS *(of this report)* UNCLASSIFIED 15a. DECLASSIFICATION/DOWNGRADING SCHEDULE

16. DISTRIBUTION STATEMENT *(of this Report)*

Approved for public release; distribution unlimited.

17. DISTRIBUTION STATEMENT *(of the abstract entered in Block 20, if different from Report)*

18. SUPPLEMENTARY NOTES

This work sponsored by the Defense Nuclear Agency under RDT&E RMSS Code B323076464 R99QAXEB06964 H2590D.

19. KEY WORDS *(Continue on reverse side if necessary and identify by block number)*

External SGEMP Analysis
Electromagnetic Response of a Sphere
Time-Dependent Electromagnetic Solution
Modal Analysis

20. ABSTRACT *(Continue on reverse side if necessary and identify by block number)*

An SGEMP skin current analysis is made for linear and non-linear source current limits. Some useful numerical data is presented. It appears that, under most circumstances, the fully time-dependent solution is necessary to describe the sphere response for only one or two modes. The remaining response may be described quasi-statically.

DD FORM 1 JAN 73 1473 EDITION OF 1 NOV 65 IS OBSOLETE

UNCLASSIFIED

SECURITY CLASSIFICATION OF THIS PAGE *(When Data Entered)*

PREFACE

I would like to thank Dr. C. Longmire and Dr. J. Gilbert for helpful discussions during a critical juncture of this work. I am indebted to Dr. C. Longmire for his encouragement during endless periods of little progress. I would also like to thank B. Marks, whose computing skill made the plots in this report possible, and Ms. Collen Hannigan who typed the report.

In discussing the results of this report with Dr. J. Gilbert of the Air Force Weapons Laboratory, I was referred to Reference 6, a relevant work. Dr. C. E. Baum of the Air Force Weapons Laboratory, the authors of Reference 6 and their associates have done a good deal of very high-quality work in the subject area of modal methods.

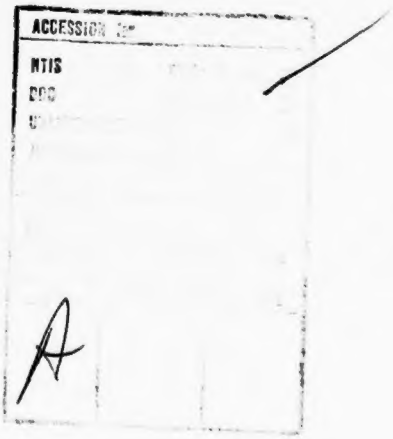

CONTENTS

ILLUSTRATIONS

SECTION 1

INTRODUCTION

This report is concerned with the analytic investigation of the electromagnetic portion of the SGEMP problem. In the SGEMP problem, photoelectrons ejected from the surface of an object are source currents for electromagnetic fields. The fields at the surface of the object are most interesting.

We investigate SGEMP phenomena using a perfectly conducting spherical model of the object. The investigation has three purposes. The first purpose is to present some directly useful data of a handbook type nature. The second purpose will be to get a deeper understanding of some of the physical aspects of the external SGEMP problem. The third purpose will be to try and gain insight into SGEMP problem analysis for an arbitrarily shaped structure.

The time-dependent analytic solution for the electromagnetic fields in space, where the source current distribution is axisymmetric and the inner boundary is a perfectly conducting sphere has been developed in Reference 1. In particular, the magnetic field at the surface of the sphere, or equivalently the skin current, is known, as a function of time, when the spatial currents are known as a function of time. The starting point for our present analysis will be the equation expressing the dependence of skin current on source currents which appears in Reference 1.

To obtain numerical data, some assumption about the mathematical nature of the source currents is necessary. Two limiting cases of the SGEMP source currents will be evaluated. The first case is that in which electron motion is unaffected by the fields they generate. This case will be called the linear limit. The second case is that in which the fields generated by the system are so strong that electrons move only a small fraction of the sphere radius, before returning to the sphere. This case will be referred to as the non-linear limit. Apart from their simplicity, these two cases may prove to be, when astutely combined, an important approximation to the general problem.

In order to make the transition from the formal solution of Reference 1 to an actual computation, mathematics is required. Section 2 will be devoted to deriving the equations necessary for the computation. Section 3 will characterize the linear limit and non-linear limit approximations for the source current. Section 4 will present the results of the computation and Section 5 will discuss the results and their relationship to the purposes of the report. Section 6 will present a summary of the report and its conclusions.

2

SECTION 2

MATHEMATICAL PRELIMINARIES

This section will be concerned only with the skin currents on the surface of a sphere. (The electric field at the surface, or equivalently the surface charge, can be obtained quite simply from the skin current and source current through a time integration.) We will be working with Equation 4-14 of Reference 1. In Reference 1 all the electromagnetic fields in space are expanded in terms of Legendre polynomials. Each Legendre coefficient for the fields is expressed as an integration over the complex ω plane and the spatial radial coordinate r'. The integrand contains the Fourier components of the Legendre coefficients of the source currents. Expression 4-14 of Reference 1 is a particular case of the general field solution. The expression is, apart from a multiplicative constant, the ℓ^{th} Legendre coefficient of the magnetic field evaluated at the surface of the sphere.

In this section we will first put Equation 4-14 of Reference 1 into a more usable form. We will then obtain some relationships which enable us to transform the integration over the complex ω domain to integrals over time. It is found to be easier to do the time integrals than the complex plane integrations. The time integral formulation also allows a deeper insight into the physics of the problem. In the final parts of this section we will find a few relations which simplify the time integrations.

Equation 4-14 of Reference 1 is

$$K_\ell(t) = \frac{i}{2\pi}\int_{-\infty}^{\infty} d\omega \left[\frac{\frac{\partial}{\partial R}(Rj_\ell(\frac{\omega}{c}R))}{\frac{\partial}{\partial R}(Rh_\ell^1(\frac{\omega}{c}R))} e^{-i\omega t} h_\ell^1(\frac{\omega}{c}R) \int_R^\infty r' h_\ell^1(\frac{\omega}{c}r')(J^r_{\ell\omega} + \frac{\partial}{\partial r'}(r'J^\theta_{\ell\omega}))dr' \right]$$

$$- \frac{i}{2\pi}\int_{\infty}^{\infty} d\omega \left[\frac{\omega}{c} j_\ell(\frac{\omega}{c}R) e^{-i\omega t} \int_R^\infty r' h_\ell^1(\frac{\omega}{c}r')(J^r_{\ell\omega} + \frac{\partial}{\partial r'}(r'J^\theta_{\ell\omega}))dr' \right] , \quad (1)$$

where K_ℓ is the ℓ^{th} Legendre coefficient of the skin current (it will be referred to as skin current magnitude); $J^r_{\ell\omega}$ and $J^\theta_{\ell\omega}$ are Fourier integral components of the ℓ^{th} Legendre coefficient of the r and θ (spherical coordinates) components of the source current $\vec{J}$; h_ℓ^1 and j_ℓ are spherical Hankel and Bessel functions respectively; R is the radius of the sphere; c is the velocity of light; ω is the frequency of the Fourier transformation and t is time. We now wish to combine the two terms in Equation 1. If we let

$$L = j_\ell - \frac{h_\ell^1 \frac{\partial}{\partial R}(Rj_\ell)}{\frac{\partial}{\partial R}(Rh_\ell^1)} , \quad (2)$$

where the argument of the spherical Hankel and Bessel functions is $(\omega/c)R$, then

$$L = \frac{[j_\ell \frac{\partial}{\partial R}(h_\ell^1) - h_\ell^1 \frac{\partial}{\partial R}(j_\ell)]R}{\frac{\partial}{\partial R}(Rh_\ell^1)} . \quad (3)$$

Using Equations 4-4 and 4-7 of Reference 1 it is easy to show that

$$L = \frac{i}{kR\frac{\partial}{\partial R}(Rh_\ell^1)} , \quad (4)$$

where

$$k \equiv \omega/c . \quad (5)$$

If we define

$$\mathcal{L}(k,r',\ell) = \frac{i}{2\pi} Lr'h_\ell^1(kr') , \quad (6)$$

then, from Equations 1, 4 and 6 we have

$$K_\ell(t) = \int_{-\infty}^{\infty} d\omega e^{-i\omega t} \int_R \mathcal{L}(J^r_{\ell\omega} + \frac{\partial}{\partial r'}(r'J^\theta_{\ell\omega}))dr' \ . \qquad (7)$$

Equation 7 is the form of Equation 1 we sought. We now derive a convenient form for $\mathcal{L}$. From Reference 2 Equations I-10 to I-12 it is easy to show that

$$h^1_\ell(kr) = \frac{(-i)^{\ell+1}}{kr} e^{ikr} \sum_{m=0}^{\ell} (i)^m Y(\ell,m)(kr)^{-m} \ , \qquad (8)$$

where $Y(\ell,m)$ is given by Equation I-13 of Reference 2:

$$\left.\begin{aligned} Y(\ell,m) &= \frac{\ell(\ell+m)\Pi_{s=1}^{m-1}(\ell^2-s^2)}{2^m m!} \ , \quad m > 0 \\ Y(\ell,0) &\equiv 1 \\ \Pi_{s=1}^{0}(\ell^2-s^2) &\equiv 1 \ . \end{aligned}\right\} \qquad (9)$$

Having found a form for h^1_ℓ, in $\mathcal{L}$, we consider L. From 8 we find

$$\frac{\partial}{\partial R}(Rh^1_\ell(kR)) = \frac{(-i)^{\ell+1}}{kR} e^{ikR}\left[\sum_{m=0}^{\ell} (i)^{m+1} Y(\ell,m)(kR)^{-(m-1)} - \sum_{m=0}^{\ell} (i)^m m Y(\ell,m)(kR)^{-m}\right]. \qquad (10)$$

By redefining the summation index in the second term of Equation 10, factoring out $(kR)^{-\ell}$, multiplying the entire bracketed expression by -i/-i, and using Equation I-43 in Reference 2 we find that

$$\frac{\partial}{\partial R}(Rh^1_\ell(kR)) = \frac{(-i)^{\ell}}{(kR)^{\ell+1}} e^{ikR}\left[(i)^{\ell+1} Y(\ell,\ell) + \sum_{m=0}^{\ell} (kR)^{\ell+1-m}(i)^m Y(\ell,m)\left(\frac{\ell(\ell+1) + m(m-1)}{\ell(\ell+1) - m(m-1)}\right)\right]. \qquad (11)$$

The expression in brackets of Equation 11 is a polynomial of degree $\ell + 1$ in kR. The roots of this polynomial determine the electric modal frequencies of the sphere. ($\partial/\partial R\ (Rh_\ell^1)$ occurs in the denominator of $\mathscr{L}$.) If we represent the q^{th} root of the polynomial of degree $\ell + 1$ by ρ_q^ℓ then

$$\Pi_{q=1}^{\ell+1}\ (kR - \rho_q^\ell) = (i)^{\ell+1}\ell\ Y(\ell,\ell) + \sum_{m=0}^{\ell} (kR)^{\ell+1-m}(i)^m Y(\ell,m)\left(\frac{\ell(\ell+1) + m(m+1)}{\ell(\ell+1) - m(m+1)}\right) . \qquad (12)$$

Substituting Equation 11 into Equation 4 and the resultant into Equation 6, together with Equations 8 and then 12 we find the needed form for $\mathscr{L}$.

$$\mathscr{L} = \frac{(kR)^\ell}{2\pi} e^{ik(r'-R)} \sum_{m=0}^{\ell} (i)^{m+1} \frac{Y(\ell,m)(kr')^{-m}}{\Pi_{q=1}^{\ell+1}\ (kR-\rho_q^\ell)} . \qquad (13)$$

By defining

$$\tau \equiv R/c , \qquad (14)$$

and

$$x \equiv r'/R , \qquad (15)$$

we can put Equation 13 into the form

$$\mathscr{L} = \frac{e^{i\omega\tau(x-1)}}{2\pi\tau} \sum_{m=0}^{\ell} (i)^{m+1} \frac{Y(\ell,m)\omega^{\ell-m}}{(\tau x)^m \Pi_{q=1}^{\ell+1}\left(\omega - \frac{\rho_q^\ell}{\tau}\right)} . \qquad (16)$$

(Eventually we want to write a dimensionless form for the skin current and Equation 16 is a start in that direction.) We now wish to combine Equations 16 and 7. Same definitions are useful. If we define

$$g_{\ell\omega}(r') \equiv J^r_{\ell\omega} + \frac{\partial}{\partial r'}\ (r' J^\theta_{\ell\omega}) , \qquad (17)$$

and

$$A_n^{\ell}(t,r') \equiv \frac{1}{2\pi}\int_{-\infty}^{\infty} \frac{g_{\ell\omega}(r')e^{-i\omega t}\omega^n d\omega}{\prod_{q=1}^{\ell+1}(\omega-\omega_q^{\ell})} , \tag{18}$$

then using the definition

$$\omega_q^{\ell} \equiv \rho_q^{\ell}/\tau , \tag{19}$$

in Equation 18, and substituting the resultant equation together with Equation 16 into Equation 7 we find that

$$K_{\ell}(t) = R \sum_{m=0}^{\ell} \left(\frac{i}{\tau}\right)^{m+1} Y(\ell,m) \int_1^{\infty} dx \, \frac{A_{\ell-m}^{\ell}(\tau(\frac{t}{\tau} - 1 + x),x)}{x^m} , \tag{20}$$

where we have substituted the variable x as defined in Equation 15, for r' in Equations 7 and 18. Equation 20 is almost the usable form of the skin current that we are seeking. One of the steps remaining is to reduce Equation 18, as used in Equation 20, to an integration over time. The following achieves that end.

In order to simplify Equation 18 we consider the following integral transform:

$$f(t) = \frac{1}{2\pi}\int_{-\infty}^{\infty} g(\omega)e^{-i\omega t}d\omega . \tag{21}$$

Taking successive derivatives of Equation 21 with respect to t we find that

$$\frac{\partial^n f(t)}{\partial t^n} = \frac{(-i)^n}{2\pi}\int_{-\infty}^{\infty} \omega^n g(\omega)e^{-i\omega t}d\omega . \tag{22}$$

(We assume, for the physical functions we are dealing with, that all the operations defined in this section are valid.) Thus we see

$$i^n \int_{-\infty}^{\infty} e^{i\omega t'} \frac{\partial^n f(t')}{\partial t'^n} dt' = \omega^n g(\omega) . \tag{23}$$

Using Equation 23 in Equation 18, where we substitute $g_{\ell\omega}(r')$ for $g(\omega)$ (the time function f will, as a consequence of this substitution, be subscripted with an ℓ) in expression 23, we find

$$A_n^{\ell} = \frac{\ell^n}{2\pi} \int_{-\infty}^{\infty} \frac{d\omega}{\prod_{q=1}^{\ell+1}(\omega-\omega_q^{\ell})} \int_{-\infty}^{\infty} e^{-i\omega(t-t')} \frac{\partial^n}{\partial t'^n} f_{\ell}(t')dt' \quad . \tag{24}$$

Interchanging the order of integration, while noting that ω_q^{ℓ} are in the lower half of the imaginary portion of the ω plane, we integrate Equation 24. Using a contour in the lower half of the ω plane for $(t - t') > 0$ (the integral is zero for $(t - t') < 0$) we find, with the theory of residues that

$$A_n^{\ell} = (i)^{n+1} \sum_{\substack{j=1 \\ j\neq q}}^{\ell+1} \frac{e^{-i\omega_j^{\ell}t}}{\prod_{q=1}^{\ell+1}(\omega_j^{\ell} - \omega_q^{\ell})} \int_0^t e^{i\omega_j^{\ell}t'} \frac{\partial^n f_{\ell}(t')}{\partial t'^n} dt' \quad . \tag{25}$$

Equation 25 can be further reduced by same knowledge of the roots ω_q^{ℓ}. The following characterization will be sufficient for our purposes. For odd ℓ (an even degree polynomial determines the roots) the roots occur in pairs so that if ω_q^{ℓ} is one root $-\omega_q^{\ell *}$ will be also. These roots describe a damped oscillation. For even ℓ, a root can occur which has no real part. This root corresponds to damping with no oscillation. Assuming that ω_1^{ℓ} and ω_2^{ℓ} are a pair of roots we look at the form of the first two terms in the sum of Equation 25:

$$\sum_{j=1}^{2} \frac{e^{-i\omega_j^{\ell}t}}{\prod_{q=1}^{\ell+1}(\omega_j^{\ell} - \omega_q^{\ell})} \int_0^t e^{i\omega_j^{\ell}t'} \frac{\partial^n f_{\ell}(t')}{\partial t'^n} dt' =$$

$$\frac{1}{2RP\omega_1^{\ell}} \left(\frac{e^{-i\omega_1^{\ell}t}}{\prod_{q=3}^{\ell+1}(\omega_1^{\ell} - \omega_q^{\ell})} \int e^{i\omega_1^{\ell}t'} \frac{\partial^n f_{\ell}(t')}{\partial t'^n} dt' - \frac{e^{+i\omega_1^{\ell *}t}}{\prod_{q=3}^{\ell+1}(-\omega_1^{\ell *} - \omega_q^{\ell})} \int e^{-i\omega_1^{\ell *}t'} \right.$$

$$\left. \frac{\partial^n f_{\ell}(t')}{\partial t'^n} dt' \right) \quad , \tag{26}$$

where RP in Equation 26 means the real part. For $\ell \geq 3$, one of the products in the denominator of the first term of Equation 26 is

$$D_{lq}^{\ell} = (\omega_l^{\ell} - \omega_q^{\ell})(\omega_l^{\ell} + \omega_q^{\ell *}) \ . \tag{27}$$

if the root ω_q^{ℓ} is one of a pair of roots. The corresponding product in the denominator of the second term is

$$F_{lq}^{\hat{\ell}} = (-\omega_l^{\hat{\ell}*} - \omega_q^{\hat{\ell}})(-\omega_l^{\hat{\ell}*} + \omega_q^{\hat{\ell}*}) \ . \tag{28}$$

It is clear that

$$D_{lq}^{*} = F_{lq} \ .$$

If ℓ is odd and all the roots occur in pairs it can be seen from Equation 28 and an examination of Equation 26 that the two terms in Equation 26 are complex conjugates of each other. Under these circumstances Equation 25 becomes

$$A_n^{\ell}(t) = (i)^{n+2} \sum_{j=1,2}^{\hat{\ell}+1} \frac{1}{\alpha_j^{\ell} \prod_{\substack{q=1,2 \\ j\neq q}}^{\ell+1} |D_{jq}^{\ell}|} \int_0^t dt' e^{\sigma_j^{\ell}(t'-t)} \frac{\partial^n f_{\ell}(t')}{\partial t'^n} \sin$$

$$\left(\alpha_j^{\hat{\ell}}(t' - t) - \sum_{\substack{q=1,2 \\ j\neq q}}^{\ell+1} \theta_{jq}^{\hat{\ell}} \right) \ , \tag{29}$$

where we have defined

$$\omega_j^{\ell} = -i\sigma_j^{\ell} + \nu_j^{\hat{\ell}} \ , \tag{30}$$

$$D_{jq}^{\ell} = |D_{jq}^{\ell}| \ e^{+i\theta_{jq}^{\ell}} \ , \tag{31}$$

and where the "2" in the summation and multiplication symbols indicates that only one root of a pair is to be used. One can obtain formulas similar

to Equation 29 if all the roots do not occur in pairs. For the source currents of this report, Equation 29 is sufficient, however. Equations 20 and 29 indicate that for each component of the skin current K_ℓ there are $\ell + 1$ terms to evaluate for each of the $(\ell + 1)/2$ pairs of frequencies. ℓ terms contain a time derivative of the current source (in Equation 29 $f_\ell(t)$ represents $J^r_\ell + \frac{\partial}{\partial r'}(r'J^\theta_\ell)$ in the actual physical system). The highest order time derivative is ℓ.

By integrating by parts in Equation 29 we can reduce the number of separate time integrals that are necessary. In the computation of the following sections it is found convenient to express the integral of $f_\ell(t')$ and the integral of $\partial f_\ell(t')/\partial t'$ in terms of the integrals of $\partial^2 f_\ell(t')/\partial t'^2$ and $\partial^3 f_\ell(t')/\partial t'^3$. We now transform the time integrals. Defining

$$\sum_{q=1,2}^{\ell+1} \theta^\ell_{jq} \equiv \theta^\ell_j \ , \tag{32}$$

in Equation 29, we have

$$I^{\ell j}_n(t) \equiv \int_0^t dt' e^{\sigma(t'-t)} \frac{\partial^n f(t')}{\partial t^n} \sin(\alpha(t'-t) - \theta) =$$

$$- \frac{\partial^{n-1} f(t)}{\partial t^{n-1}} \sin\theta - \int_0^t \frac{\partial^{n-1} f(t')}{\partial t^{n-1}} e^{\sigma(t'-t)}(\sigma \sin(\alpha(t' - t) - \theta)$$

$$+ \alpha\cos(\alpha(t' - t) - \theta))dt' \ , \tag{33}$$

where we have assumed that for $t < 0$ the function and all its derivatives are equal to zero. We have dropped the subscript ℓ on $f(t)$ and the superscript ℓ and subscript j on σ, α and θ for convenience. Making a partial integration in Equation 33 we have

$$I_n^{\ell j}(t) = -\frac{\partial^{n-1} f(t)}{\partial t^{n-1}} \sin\theta - \frac{\partial^{n-2} f(t)}{\partial t^{n-1}} (\alpha\cos\theta - \sigma\sin\theta)$$

$$+ \int_0^t \frac{\partial^{n-2}}{\partial t^{n-2}} f(t') e^{\sigma(t'-t)} ((\sigma^2 - \alpha^2)\sin(\alpha(t' - t) - \theta)$$

$$+ 2\sigma\alpha\cos(\alpha(t' - t) - \theta))dt' \ . \qquad (34)$$

By combining Equation 33 with n = 2 and Equation 34' with n = 3 in such a way as to remove the integral of $\frac{\partial f}{\partial t} \cos(\alpha(t' - t) - \theta)$ we find

$$I_1^{\ell j} = \frac{1}{|\tilde{\omega}|^2} \left\{ -\frac{\partial^2 f(t)}{\partial t^2} \sin\theta - \frac{\partial f(t)}{\partial t} (\sigma\sin\theta + \alpha\cos\theta) \right.$$

$$\left. - I_3^{\ell j} - 2\sigma I_2^{\ell j} \right\} \ , \qquad (35)$$

where

$$|\tilde{\omega}| \equiv \sigma^2 + \alpha^2 \ . \qquad (36)$$

Similarly by conbining (33), with n = 1, and Equation 34, with n = 2, together with Equation 35 we find

$$I_0^{ij} = \frac{1}{|\tilde{\omega}|^2} \left[\frac{2\sigma}{|\tilde{\omega}|^2} \frac{\partial^2 f(t)}{\partial t^2} \sin\theta \right.$$

$$+ \frac{\partial f(t)}{\partial t} \left(\left(\frac{2\sigma^2}{|\tilde{\omega}|^2} - 1 \right) \sin\theta + \frac{2\sigma\alpha}{|\tilde{\omega}|^2} \cos\theta \right)$$

$$- F(t)[\sigma\sin\theta + \alpha\cos\theta]$$

$$\left. + \frac{2\sigma}{|\tilde{\omega}|^2} I_3^{ij} + \left(\frac{4\sigma^2}{|\tilde{\omega}|^2} - 1 \right) I_2^{ij} \right] \ . \qquad (37)$$

Equations 35 and 36 are those necessary for our purposes. As a finale for this section we put Equation 20 into a dimensionless form. The dimensionless form is convenient for comparing results.

Beginning with Equation 29 and defining a dimensionless time by

$$\bar{t} = t/\tau \ , \tag{38}$$

where τ is defined by Equation 14 we find that

$$A_n^{\ell}(t) = (i)^{n+1}(\tau)^{\ell-n+1} \sum_{j=1,2}^{\ell+1} \frac{1}{\bar{\alpha}_j^{\ell} \prod_{\substack{q=1,2 \\ j\neq q}}^{\ell+1} |\bar{D}_{jq}^{\ell}|} \int_0^{\bar{t}} d\bar{t}' \left(e^{\bar{\sigma}_j^{\ell}(\bar{t}'-t)} \right.$$

$$\left. \frac{\partial^n f_{\ell}(\bar{t}')}{\partial \bar{t}'^n} \sin(\bar{\alpha}_j^{\ell}(\bar{t}' - \bar{t}) - \theta_j^{\ell}) \right) \ , \tag{39}$$

where

$$\bar{\alpha}_j^{\ell} = \tau \alpha_j^{\ell} \ , \tag{40}$$

$$\bar{\sigma}_j^{\ell} = \tau \sigma_j^{\ell} \ , \tag{41}$$

and

$$\bar{D}_{jq}^{\ell} = (\rho_j^{\ell} - \rho_q^{\ell})(\rho_j^{\ell} - \rho_q^{\ell *}) \ , \tag{42}$$

where ρ_j^{ℓ} is defined by Equation 19. It should be noted that θ_j^{ℓ} does not change with this transformation and $\bar{\sigma}_j^{\ell}$ and $\bar{\alpha}_j^{\ell}$ are the imaginary and real parts of ρ_j^{ℓ} respectively. If we normalize $f(\bar{t})$ where we define

$$f_0 \equiv \int f(t)dt = \tau \int f(\bar{t})d\bar{t} \equiv \tau \bar{f}_0 \tag{43}$$

$$\bar{f}(\bar{t}) \equiv f(\bar{t})/f_0 \ , \tag{44}$$

then

$$A_n^{\ell}(t) = (i)^{n+2}(\tau)^{\ell-n} f_0 \bar{A}_n^{\ell}(\bar{t}) \quad , \tag{45}$$

where

$$\bar{A}_n^{\ell}(\bar{t}) \equiv \sum_{j=1,2}^{\ell+1} \frac{1}{\bar{\alpha}_j^{\ell} \Pi_{q-1,2}^{\ell+1} |\bar{D}_{jq}^{\ell}|} \int_0^{\bar{t}} d\bar{t}' \left(e^{\bar{\sigma}_j^{\ell}(\bar{t}'-\bar{t})} \right.$$

$$\left. \frac{\partial^n \bar{f}_{\ell}(\bar{t}')}{\partial \bar{t}'^n} \sin(\bar{\alpha}_j^{\ell}(\bar{t}' - \bar{t}) - \theta_j^{\ell}) \right) \quad . \tag{46}$$

Substituting (45) into (20) where we make the correspondence

$$\bar{f}_{\ell}(\bar{t}') \rightarrow \overline{J_{\ell}^r(\bar{t}', r') + \frac{\partial}{\partial r'}\left(r' J_{\theta}^r(\bar{t}', r')\right)} \quad , \tag{47}$$

so that actually $\bar{A}_n^{\ell}(\bar{t})$ also contains the variable r', besides $\bar{t}$, we find that

$$K_{\ell}(t) = -\, c f_0 \sum_{m=0}^{\ell} (i)^{\ell+1} Y(\ell, m) \int_1^{\infty} dx \; \frac{\bar{A}_{\ell-m}(\bar{t}-(1+x), x)}{x^m} \quad , \tag{48}$$

where we have used the definitions expressed by Equations 14 and 15. Equation 48 together with Equation 46 are the dimensionless forms we seek.

SECTION 3

SOURCE CURRENT APPROXIMATION

In this section we will discuss the linear and non-linear limits for the source currents. The end of this discussion will be the arrival at a set of expressions, to be evaluated, which include all the parameters of the specific source currents to be used.

Two approximations are shared by both the linear and non-linear limits. These approximations are common to many "Maxwell Solver-Particle Pusher" computer code simulations of SGEMP. As usual, these approximations are made to simplify the labor involved in the calculations, and also because their affect on the physics of a real problem is not believed to be too appreciable. The first approximation assumes that electrons are emitted only perpendicular to the emitting surface. That is

$$J^{\theta} = 0 \ , \tag{49}$$

for our sphere problem. More accurate computer calculations of SGEMP effects assume electrons are emitted with a cosine distribution, with respect to the normal to the surface. Although detailed studies have apparently not been performed, the opinion of some workers in the field is that simulation with the two types of emission yields similar results. An upper bound of 30 percent, on the difference in magnitude of skin currents generated by these two types of emission is sometimes, unofficially, quoted.

A second approximation is that emission from all points on the emitting half sphere begins simultaneously. This approximation is expressed as

$$J^r = H(\pi/2 - \theta)\mu(r,t) \ , \tag{50}$$

where H is a step function and μ is a function of the radial spatial coordinate and time. The range of θ variable for the half sphere that is emitting is $0 < \theta < \pi/2$. In a typical physical problem a plane wave of X rays strikes a point of the sphere ($\theta = 0$); all the points of the half sphere begin emitting after a time R/c (the time it takes light to cross a half sphere). For those sources whose effective time duration is much larger than R/c, Equation 50 is clearly a valid approximation. For those sources who's effective time duration is comparable or smaller than R/c, the validity of the approximation is not certain.

A direct consequence of Equation 50 is that the electromagnetic fields may be expressed in terms of a series of odd order Legendre polynomials. The proof is simple. Expanding $H(\pi/2 - \theta)$ in terms of Legendre polynomials we have:

$$H(\pi/2 - \theta) = \sum_{\ell=0}^{\infty} a_\ell P_\ell(\cos\theta) \ , \tag{51}$$

where

$$a_\ell = \frac{2\ell + 1}{2} \int_1^0 P_\ell(x)dx \ , \tag{52}$$

and

$$x \equiv \cos\theta \ . \tag{53}$$

From the orthogonality properties of the Legendre polynomials ($P_0(x)$ is a constant) we know that

$$\int_{-1}^{0} P_\ell(x)dx + \int_0^1 P_\ell(x)dx = 0 \quad , \quad \ell \geq 1 \ . \tag{54}$$

But, since $P_\ell(x)$ is an even or odd function of x when ℓ is even or odd,

$$\int_{-1}^{0} P_\ell(x)dx = (-1)^\ell \int_{0}^{1} P_\ell(x)dx \ . \tag{55}$$

From Equations 55 and 54 it is clear that a_ℓ in Equation 52 is equal to zero for even ($\ell \neq 0$). Since we need a_ℓ for our computations we now find their numerical values. Noting that[3]

$$\int_{1}^{0} P_\ell(x)dx = \frac{(2n - 1)!!(-1)^{n+1}}{2^{n+1}(n + 1)!} \ , \tag{56}$$

where

$$n \equiv \frac{\ell - 1}{2} \ , \tag{57}$$

we have, after substituting Equation 56 into Equation 52

$$a_\ell = \frac{(4n + 3)}{2^{n+2}} \frac{(2n - 1)!!}{(n + 1)!} (-1)^{n+1} \ . \tag{58}$$

In this report, for both the linear and non-linear limit, we will be concerned only with the first two terms in the infinite series for the skin current, that is, the terms labeled by $\ell = 1$ and 3 ($n = 0$ and 1). From Equation 58 we see that

$$a_1 = - 3/4 \ , \tag{59}$$

$$a_2 = + 7/16 \ . \tag{60}$$

Looking at Equation 46 we see that we need the numerical values of $|\bar{D}^\ell_{jq}|$, θ^ℓ_j, $\bar{\alpha}^\ell_j$ and $\bar{\sigma}^\ell_j$, when ℓ is equal to 3 and $\bar{\alpha}^\ell_j$ and $\bar{\sigma}^\ell_j$ when ℓ is equal to 1, for our computations, with either the linear or non-linear limits for the sources. We begin with $\ell = 1$ and find the needed values.

The equation for $\bar{\alpha}^1$ and $\bar{\sigma}^1$ (the subscript j is suppressed since only one pair of roots exists) is given by Equation 12 where

$$\rho \equiv kR \ . \tag{61}$$

Using the definition of $Y(\ell,m)$ provided by Equation 9 we see that the solution of

$$-1 + i\rho + \rho^2 = 0 \ , \tag{62}$$

provides the roots

$$\begin{aligned} \bar{\alpha}^1 &= \sqrt{3/4} \ , \\ \bar{\sigma}^1 &= 1/2 \ . \end{aligned} \tag{63}$$

Equation 62 and its solution is the same as those of Reference 4. The equation describing the roots for $\ell = 3$ is obtained in the same way as the $\ell = 1$ equation. It is

$$\rho^4 + i6\rho^3 - 21\rho^2 - i45\rho + 45 = 0 \ . \tag{64}$$

The solution of Equation 64 is found by numerically solving a cubic equation. One eventually finds that

$$\begin{aligned} &\bar{\alpha}_1^3 = .870569 \ , \ \bar{\alpha}_2^3 = 2.75785 \ , \\ &\bar{\sigma}_1^3 = 2.15713 \ , \ \bar{\sigma}_2^3 = .842862 \ , \end{aligned} \tag{65}$$

to six places. Using the definitions expressed by Equation 42, where $\bar{D}_{jq}^{\ell}$ is equal to $|\bar{D}_{jq}^{\ell}|e^{i\theta_{jq}^{\ell}}$, we find, after reference to Equations 19, 30, 40 and 41, that

$$\begin{aligned} &|\bar{D}_{21}^3| = |\bar{D}_{12}^3| = 8.87527 \\ &\theta_{12}^3 = -2.88081 \text{ radians} \\ &\theta_{21}^3 = .955811 \text{ radians} \ . \end{aligned} \tag{66}$$

LINEAR LIMIT

As monoenergetic electrons, of velocity v, leave the sphere their flux decreases by a factor of $(R/r')^2$, where R is the sphere radius and r' is the radial coordinate. If $f(t)(2\pi R^2)$ is the total number of electrons leaving the half sphere at time t then that same number appears at the half sphere located at r' but at a time $t - (r' - R')/v)$ later[5]. That is from Equations 50 and 51

$$J_\ell^r = a_\ell (R/r')^2 f(t - (r' - R)/v) \ . \tag{67}$$

Equation 67 expresses the linear limit, source approximation. We will want to calculate and plot the skin currents, due to a source of this form, for a number of different velocities. With this end in mind we substitute Equations 49 and 67 into Equation 47 and the result into (46). We find, after utilizing Equations 35, 36, 37, 63, 65, and 66 and after doing some laborious numerical calculations, that

$$K_1(t) = cf_0(-3/4) \int_1^\infty \frac{dx}{x^2} \left(\left(-1 + \frac{1}{x}\right) F_{13}^1 - F_{12}^1 \right) \frac{1}{\bar{\alpha}'} - \frac{\bar{f}(y)}{x} + \left(-1 + \frac{1}{x}\right) \frac{\partial \bar{f}(y)}{\partial \bar{t}} \Bigg), \tag{68}$$

and

$$K_3(t) = -cf_0\left(\frac{7}{16}\right) \int_1^\infty \frac{dx}{x^2} \Bigg[F_{13}^3 \left(.129424 - \frac{.358771}{x^2} + \frac{.286047}{x^3}\right) + F_{23}^3 \left(.040855 - \frac{.073690}{x^2} + \frac{.014937}{x^3}\right) + F_{12}^3 \left(.776544 - \frac{1.54783}{x^2} + \frac{.875314}{x^3}\right) + F_{22}^3 \left(.245130 - \frac{.124222}{x^2} - .048510\right) + \frac{1}{3} \frac{\partial \bar{f}(y)}{\partial \bar{t}} \left(\frac{1}{x^2} - \frac{1}{x^3}\right) + \frac{1}{3} \bar{f}(y) \frac{1}{x^3} + \frac{\partial^2 \bar{f}(y)}{\partial t^2} \left(\frac{.032313}{x^2} - \frac{.061551}{x^3}\right) \Bigg] . \tag{69}$$

where

$$y \equiv \bar{t} - (x - 1)(1 + \gamma^{-1}) \quad , \quad \gamma \equiv v/c \ , \tag{70}$$

$$F_{jk}^{\ell}(x,t) \equiv \int_0^y dt' \, \frac{\partial^k}{\partial t'^k} \bar{f}(t') e^{\bar{\sigma}_j^{\ell}(\bar{t}'-y)} \sin(\alpha_j^{\ell}(\bar{t}' - y) - \theta_j^{\ell}) \ , \tag{71}$$

and

$$f_0 = \int_0^{\infty} f(t)dt \ , \tag{72}$$

(the total amount of charge/cm^2 leaving the conducting surface) where

$$\bar{f}(t) \equiv (f(t)\tau)/f_0 \ . \tag{73}$$

The $\frac{1}{3}$ in expression 69 has six place accuracy. Note that f(t) is defined by Equation 67 and also that the definitions expressed by Equations 15 and 38 have been used in deriving Equations 68 and 69. The other symbols used under the integral sign of Equation 71, to be used in Equations 68 and 69, can be obtained from Equations 63, 65 and 66, where we note, however, that θ^1 is equal to zero. Equation 70 defines a dimensionless retarded time y with an effective velocity of retardation c_e, where

$$\frac{c_e}{c} \equiv 1 + \gamma^{-1} \ . \tag{74}$$

Both the time for a charged particle to get from R to r', and the time for light to travel from r' to R are included in y. The reason y occurs in expressions (68), (69) and (71) rather than $\bar{t} - (x - 1)$ can be seen by noting that the Fourier transform of $f(t - \frac{(r'-R)}{v})$ is given by

$$e^{+i\omega(\frac{r'-R}{v})} \int_{-\infty}^{\infty} e^{i\omega t} f(t)dt \ ,$$

or is equal to the Fourier transform of f(t) multiplied by the factor $e^{+i\omega((r'-R)/v)}$. This factor has the same form as the exponential factor $e^{ik(r'-R)}$ in Equation 13 and so (r'-R)/v would appear in the subsequent equations of Section 2 in the same way that (r'-R)/c appears.

More useful forms of Equations 68 and 69—from a computational standpoint—can be found by partially integrating the F^{ℓ}_{13} terms in these equations while also expanding the sine and cosine terms in Equation 69. The resulting equations are

$$K_1(t) = cf_0 \frac{3}{4} \int_1^{\infty} \frac{dx}{x^2} \left(\frac{\bar{f}(y)}{x} + \left(1 - \frac{1}{x}\right) \frac{\partial \bar{f}}{\partial \bar{t}} (y) \right.$$

$$\left. - \frac{1}{\sqrt{3}} \left(1 + \frac{1}{x}\right) C^1_{12} + \left(1 - \frac{1}{x}\right) S^1_{12} \right) , \tag{68'}$$

and

$$K_2(t) = - cf_0 \left(\frac{7}{16}\right) \int_1^{\infty} \frac{dx}{x^2} \left(\frac{1}{3} \bar{f}(y) \frac{1}{x^3} + \frac{1}{3} \frac{\partial \bar{f}(y)}{\partial \bar{t}} \left(\frac{1}{x^2} - \frac{1}{x^3} \right) \right.$$

$$+ S^3_{12} \left(.451492 - \frac{.667222}{x^2} + \frac{.185332}{x^3} \right) + C^3_{12} \left(.237098 - \frac{.501317}{x^2} + \frac{.307195}{x^3} \right) \tag{69'}$$

$$\left. + S^3_{22} \left(-.029531 - \frac{.130158}{x^2} + \frac{.068899}{x^3} \right) + C^3_{22} \left(-.237098 + \frac{.167983}{x^2} + \frac{.026138}{x^3} \right) \right) ,$$

where

$$\left. S^{\ell}_{jk} = \int_0^{y} \frac{\partial^k f(\bar{t}')}{\partial \bar{t}'^k} e^{\bar{\sigma}^{\ell}_j (\bar{t}'-y)} \sin \bar{\alpha}^{\ell}_j (\bar{t}'-y) d\bar{t}' \right\}$$

and (71')

$$\left. C^{\ell}_{jk} = \int_0^{y} \frac{\partial^k f(\bar{t}')}{\partial \bar{t}'^k} e^{\bar{\sigma}^{\ell}_j (\bar{t}'-y)} \cos \bar{\alpha}^{\ell}_j (\bar{t}'-y) d\bar{t}' \right\} .$$

In general photoelectrons leaving the spherical surface are not monoenergetic but are described by a spectrum of velocities. If f(t) is known for each of the different electron velocities then $K_{\ell}(t)$ can be summed for each of the individual velocities to obtain the effect of the total

spectrum. If all the photoelectrons have the same time history, as it is usually assumed in SGEMP work, the total skin current calculation is simpler.

NON-LINEAR LIMIT

In this limit we assume the fields generated are so strong that electrons ejected from the surface move only a small fraction of the radius before returning. Under these circumstances the spatial integration in Equation 48, the integration over x, is basically that of a delta function at x = 1, that is the integrand is evaluated at x equal to 1. The physical quantity that results from the spatial integration can be viewed as the time rate of change of a dipole moment per unit area. The dipole moment has a time history f(t). As in the linear limit, one can view the total skin current as coming from a sum of the effects of different dipole moments produced by several groups of monoenergetic electrons with different time histories. One could also view the dipole moment of the spatial integrations as the total dipole moment of several groups of electrons with the same time history. This latter view is closer to the usual SGEMP assumption. Integrating an x in Equations 68' and 69' as though the integrand contained $\delta(x - 1)$ we find the skin current is $\bar{f}(\bar{t})$ (see Equation 73 for a definition of $\bar{f}(\bar{t})$):

$$K_1(t) = cf_0 \frac{3}{4} \left(\bar{f}(\bar{t}) + \frac{2}{\sqrt{3}} S^1_{12}(\bar{t})\right) , \tag{75}$$

$$\left.\begin{aligned} K_3 = - cf_0 \frac{7}{16} \Big(&\frac{1}{3} \bar{f}(\bar{t}) - .030397\, S^3_{12}(\bar{t}) \\ &+ .042976\, C^3_{12}(\bar{t}) - .090790\, S^3_{22}(\bar{t}) \\ &- .04296\, C^3_{22}(\bar{t})\Big) . \end{aligned}\right\} \tag{76}$$

Together with Equations 70, 71' (setting x = 1), 63 and 65, Equations 75 and 76 are those needed for the non-linear limit. We will use these equations to compute skin currents for various $\overline{f}(\overline{t})$.

It should be noted that in arriving at Equations 75 and 76 we assumed that the source currents had the form $\delta(x - 1)$. This assumption becomes invalid for ℓ greater than some finite integer "N," because the wavelengths of the oscillations will become comparable to and smaller than the dipole thickness. To make the series of K_ℓ convergent, in a mathematical sense, for the non-linear limit, an integration over x would have to be performed for $\ell > N$.

SECTION 4

RESULTS

We begin first with the non-linear limit since it is simpler and consequently demonstrates the implications of the theory more clearly. To do the computations it remains only to choose a time history (pulse shape) and substitute it into Equations 75 and 76. A simple time history, although not necessarily adequate, physically, is a triangular pulse which, starting from t = 0, reaches its maximum in $t_f/2$ and is over at t_f (t_f will be referred to as pulse length). In terms of the dimensionless time and a normalized pulse we have

$$\begin{aligned} \bar{f}(\bar{t}) &= \beta\bar{t} \quad 0 < \bar{t} < \bar{t}_f/2 \\ \bar{f}(\bar{t}) &= \beta(\bar{t}_f - \bar{t}) \quad \bar{t}_f/2 < t < \bar{t}_f \\ \bar{f}(\bar{t}) &= 0 \quad \bar{t}_f < \bar{t} < 0 \ , \end{aligned} \tag{77}$$

$$\frac{\partial \bar{f}}{\partial \bar{t}} = \beta(H(0) - 2H(\bar{t} - \bar{t}_f/2) + H(\bar{t} - \bar{t}_f)) \ , \tag{78}$$

$$\frac{\partial^2 \bar{f}}{\partial \bar{t}^2} = \beta(\delta(0) - 2\delta(\bar{t} - \bar{t}_f/2) + \delta(\bar{t} - \bar{t}_f)) \ , \tag{79}$$

$$\frac{\partial^3 \bar{f}}{\partial \bar{t}^3} = \beta \frac{\partial}{\partial \bar{t}} \delta(0) - 2 \frac{\partial}{\partial \bar{t}} \delta(\bar{t} - \bar{t}_f/2) + \frac{\partial}{\partial \bar{t}} \delta(\bar{t} - \bar{t}_f)) \ , \tag{80}$$

Where

$$\bar{t}_f = t_f/\tau \ , \tag{81}$$

$$\beta \equiv (\bar{t}_f/2)^{-2} \ , \tag{82}$$

H is a step function and δ is a delta function. Substituting Equations 77 through 80 into Equations 75 and 76 and plotting the results for various values of $\bar{t}_f$ we obtain Figures 1, 2 and 3. We have divided K_1 by the factor $c\frac{3}{4}f_0$ and also by the factor $\beta\bar{t}_f$ to obtain the ordinate values. Figure 1 is a plot of Equation 75 for the above defined $\bar{f}(\bar{t})$. As will be explained in the next section under "Low and High Frequency Limits," the term $c\frac{3}{4}f_0\bar{f}(\bar{t})$, in Equation 75, is the quasi-static limit of the $\ell = 1$ component of the skin current. In Figure 1 the quasi-static limit appears, for any pulse length, as a triangle of height .5 with a width of 1.0. The plots demonstrate how the actual skin current differs from the quasi-static limit for the $\bar{t}_f$ values of .1, .5, 1, 5 and 10. Equation 71' defines the term S^1_{12} which appears in Equation 75. Setting $\bar{\sigma}^{\ell}_j$ equal to zero in that expression yields the graph labeled (1,0) in Figure 1—the pulse length $\bar{t}_f$ is 1 and there is no damping. The plots of Figure 2 are similar to those of Figure 1. Two curves are plotted along with the quasi-static limit. Both are plots of Equation 75 with a pulse length of 12. One plot contains the damping in the S^1_{12} term the other, labeled (12,0) does not.

The quasi-static limit for Equation 76 is the term $-c\frac{7}{16}f_0\frac{1}{3}\bar{f}(\bar{t})$. Using the triangular pulse function defined above for $\bar{f}(\bar{t})$ in Equation 76 we find values for the plots of Figure 3. In Figure 3 the ordinate values of skin current magnitude are divided by $-c\frac{7}{48}f_0\beta\bar{t}_f$ while the abscissa is $\bar{t}/\bar{t}_f$. As in Figures 1 and 2, the quasi-static limit for $\ell = 3$ appears as a triangle of height .5 and width 1. The pulse widths considered were $\bar{t}_f$ = .1, .5, 1, 5 and 10.

The triangular pulse defined by Equations 77 is discontinuous. Figure 4 is a plot of the $\ell = 1$ skin current response for a smooth function with a continuous first derivative at the beginning and at the end of the pulse. The time history is defined as follows:

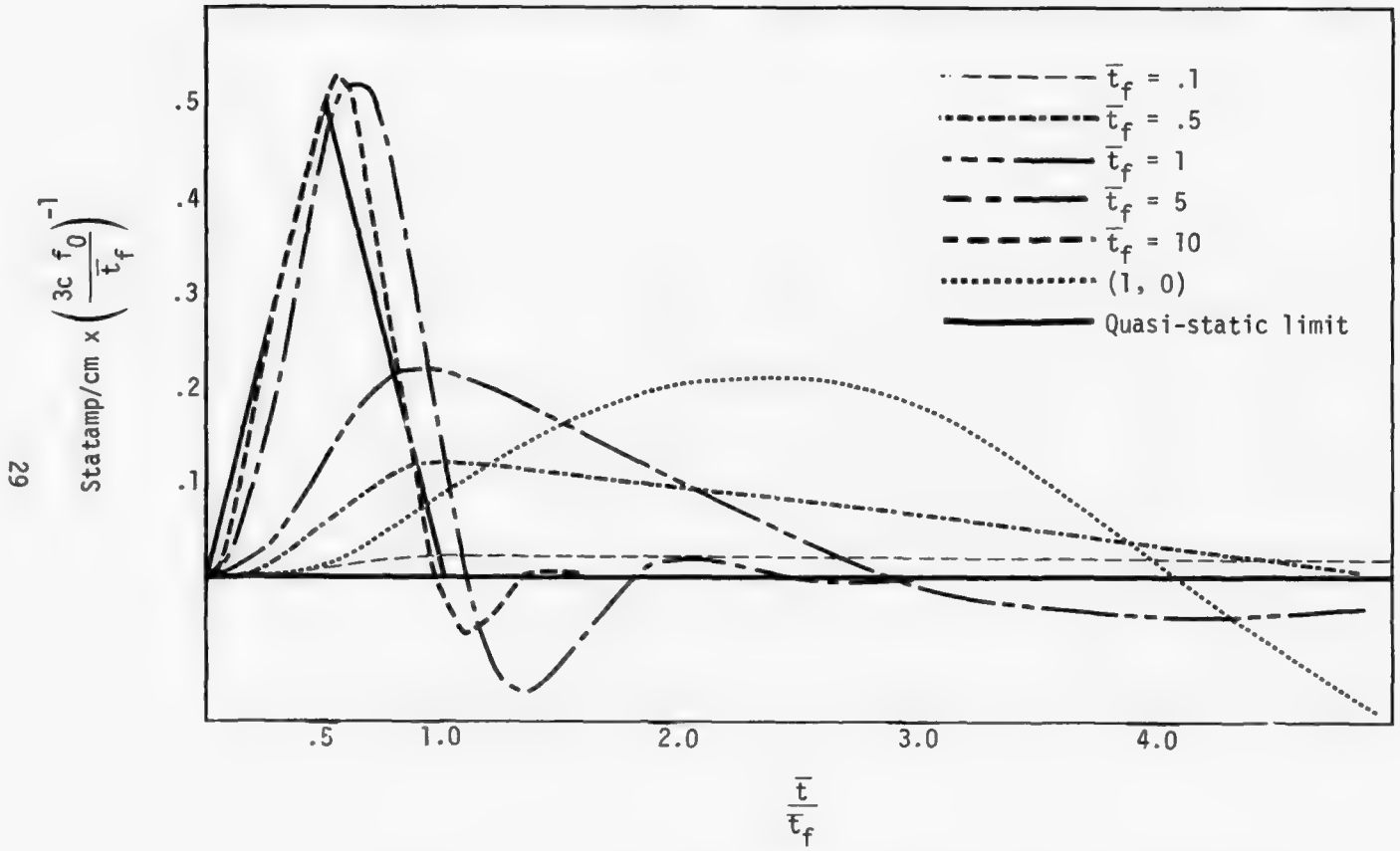

Figure 1. ℓ = 1, non-linear limit, triangle excitation. Normalized skin current magnitude vs. normalized time.

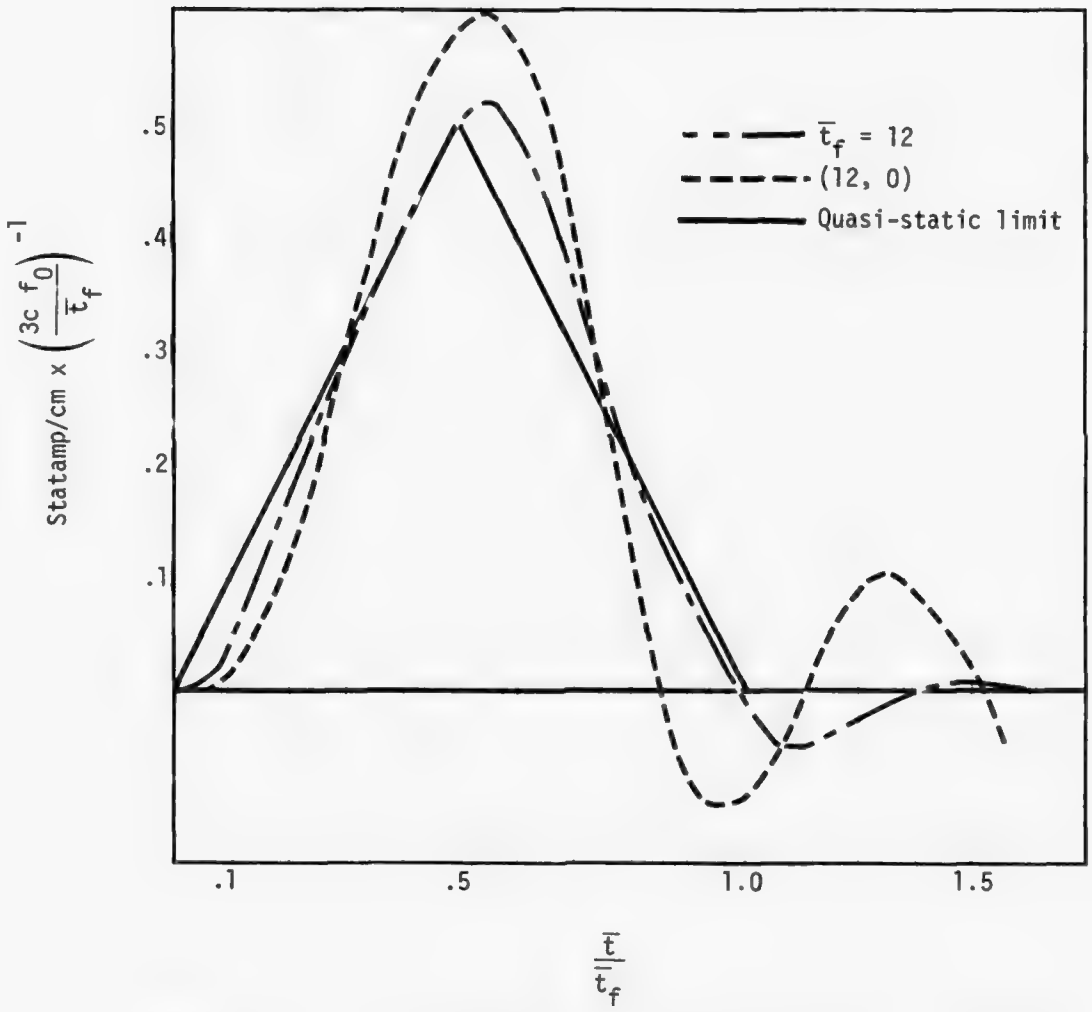

Figure 2. ℓ = 1, non-linear limit, triangle excitation. Normalized skin current magnitude vs. normalized time.

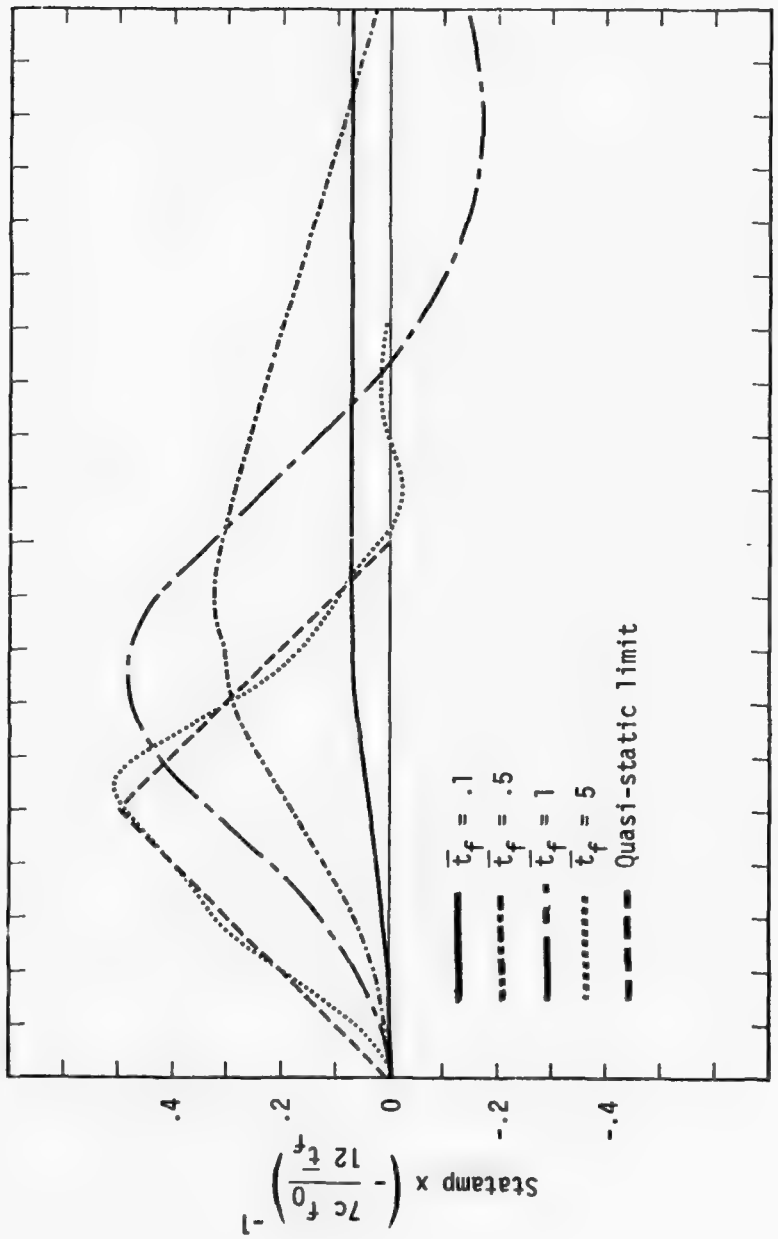

Figure 3. $\ell = 3$, non-linear limit, triangle excitation. Normalized skin current magnitudes vs. normalized time.

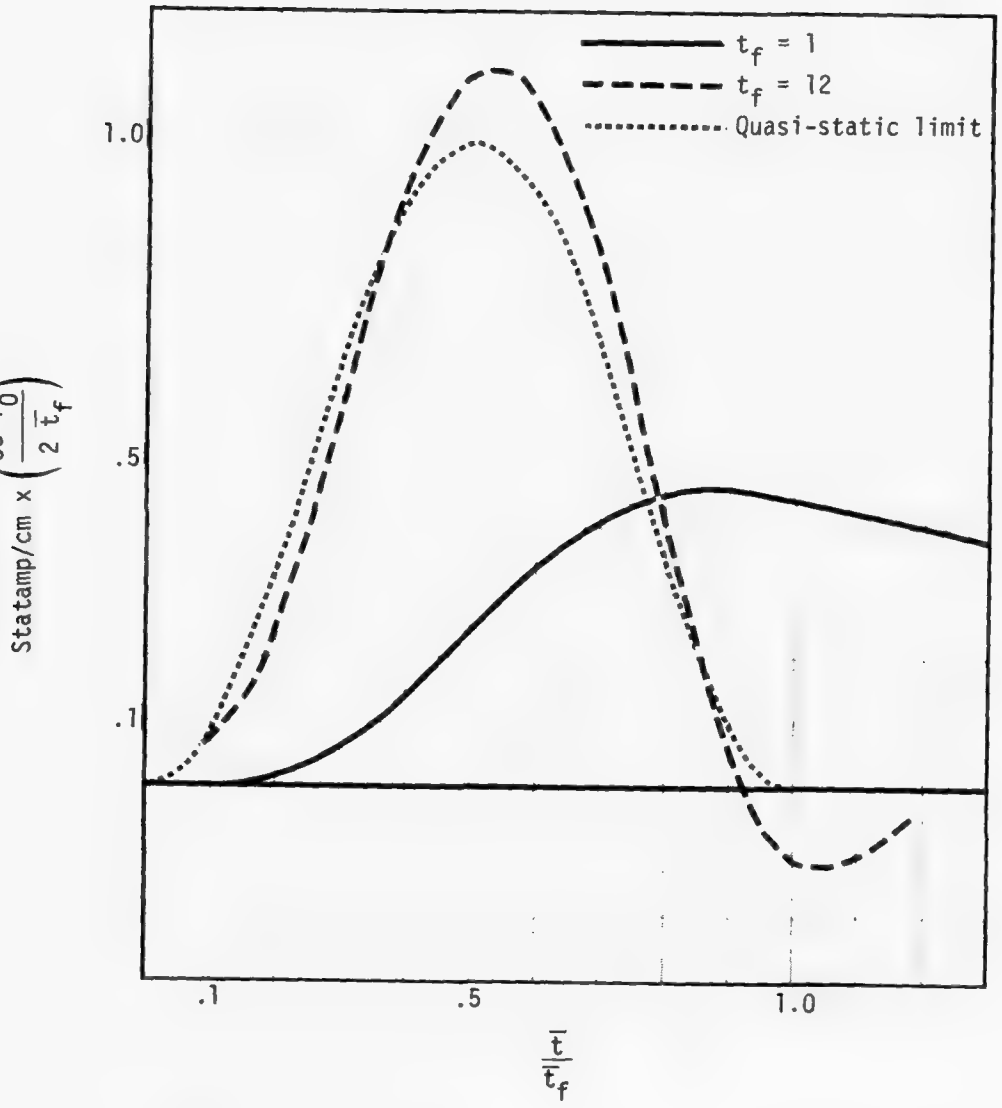

Figure 4. ℓ = 1, non-linear limit, $\sin^2$ excitation. Normalized skin current magnitude vs. normalized time.

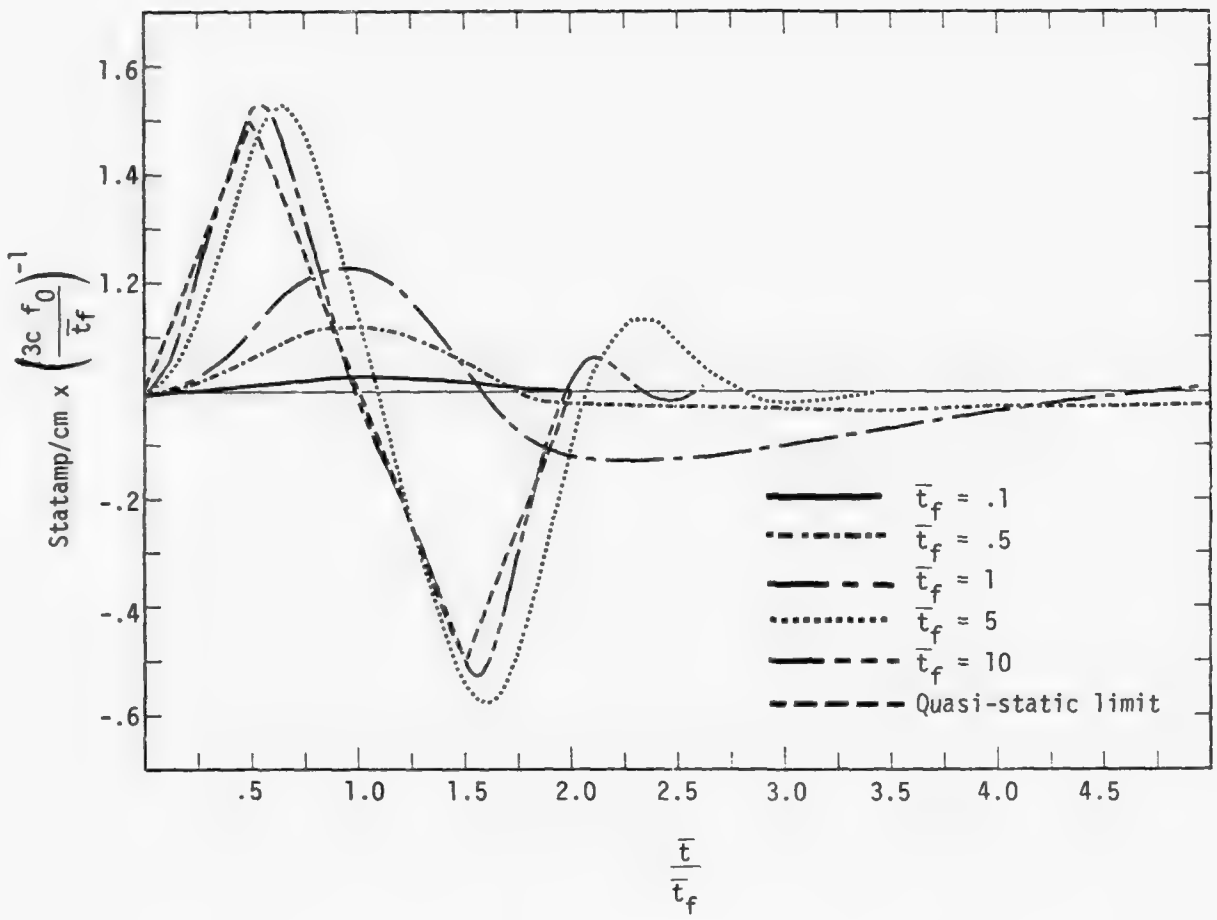

Figure 5. ℓ = 1, non-linear limit, double triangle excitation. Normalized skin current magnitude vs. normalized time.

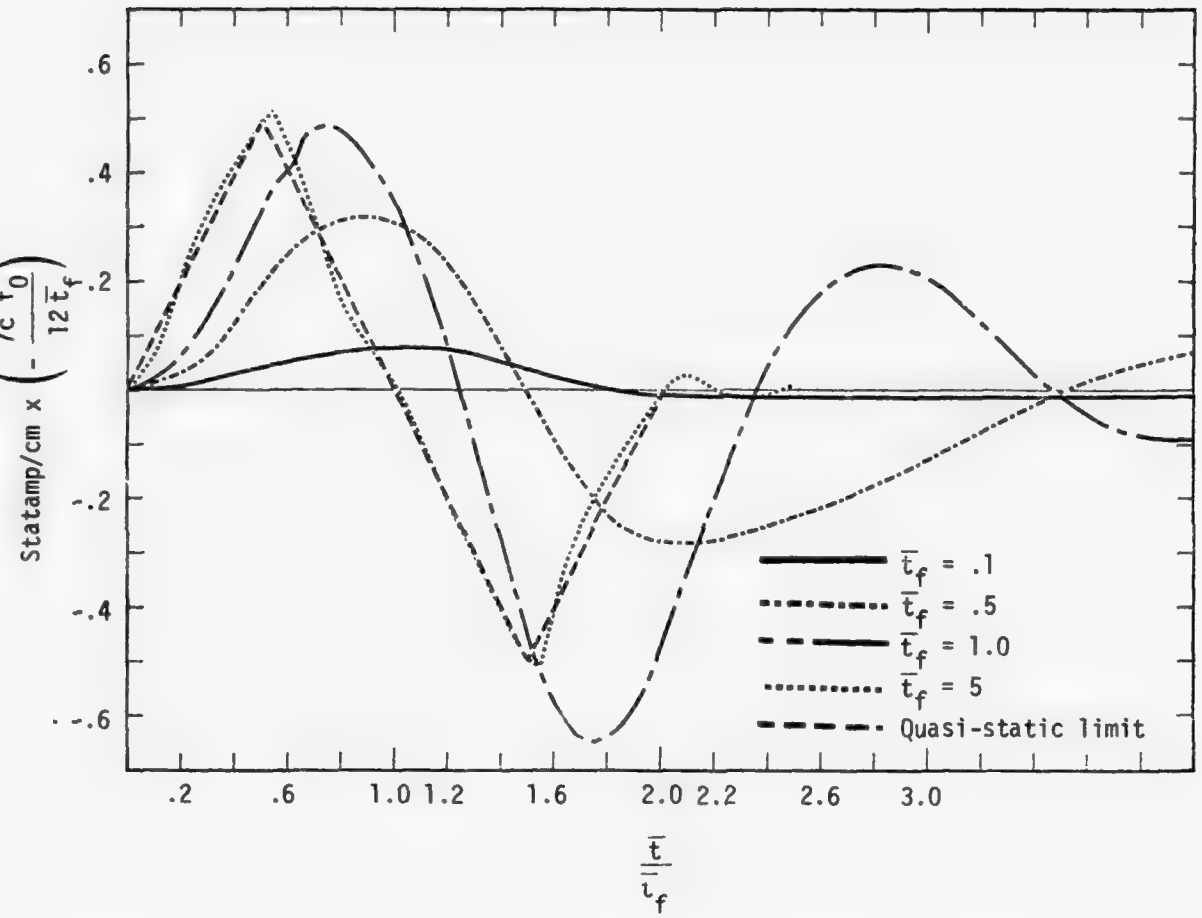

Figure 6. ℓ = 3, non-linear limit, double triangle excitation. Normalized skin current magnitude vs. normalized time.

$$\bar{f}(\bar{t}) = \beta \sin^2 \pi(\bar{t}/\bar{t}_f) \ , \tag{83}$$

$$\beta = \left(\frac{\bar{t}_f}{2}\right)^{-1} \ . \tag{84}$$

Two pulse lengths, $t_f = 1, 12$, are compared with the quasi-static limit in Figure 4. It is of interest to compare the deviations from the quasi-static limit, for the corresponding pulse lengths in Figures 1, 2 and 4. Another type of pulse shape can be defined by a double triangle as follows:

$$\begin{aligned}
\bar{f}(\bar{t}) &= \beta\bar{t} \quad 0 < \bar{t} < \bar{t}_f/2 \ , \\
\bar{f}(\bar{t}) &= \beta(t_f - t) \quad t_f/2 < \bar{t} < \tfrac{3}{2} t_f \ , \\
\bar{f}(\bar{t}) &= \beta(2t_f - t) \quad \bar{t}_f/2 < \bar{t} < 2\bar{t}_f \ , \\
\bar{f}(\bar{t}) &= 0.0 \quad 2\bar{t}_f < \bar{t} \ ,
\end{aligned} \tag{85}$$

where

$$\beta \equiv (\bar{t}_f/2)^2 \ , \tag{86}$$

and f_0 in Equations 75 and 76 is the time integral of the actual, non-normalized, time function over the range $0 < t < \tau\bar{t}_f/2$. Plots of skin current magnitudes produced by the latter time history appear in Figures 5 and 6. They are plotted in a manner similar to the plotting of the single triangle time history.

Plots of $\ell = 1$ and $\ell = 3$ skin current magnitudes, for the linear limit, appear in Figures 7 through 28. The skin current values for Figures 7 through 26 were calculated by substituting the triangular time history, defined by Equations 77, into Equations 68' and 69' and performing a spatial integration in x. Five pulse lengths, $\bar{t}_f$, and five v/c ratios are used. The pulse lengths are .1, .5, 1.0, 5 and 10. The v/c values are .063, .136, .186, .239 and 1.0. The ordinate values for the $\ell = 1$ plots are the skin current divided by $c\,\frac{3}{4} f_0$; the ordinate values for the $\ell = 3$ plots are the skin current divided by $-c\,\frac{7}{16} f_0 \frac{4}{3} \frac{1}{3}$. Sometimes the ordinate values of skin current magnitudes are also multiplied by 10 or 10^2. As in Figures 1 through 6 a comparison is made with the quasi-static limit. The skin

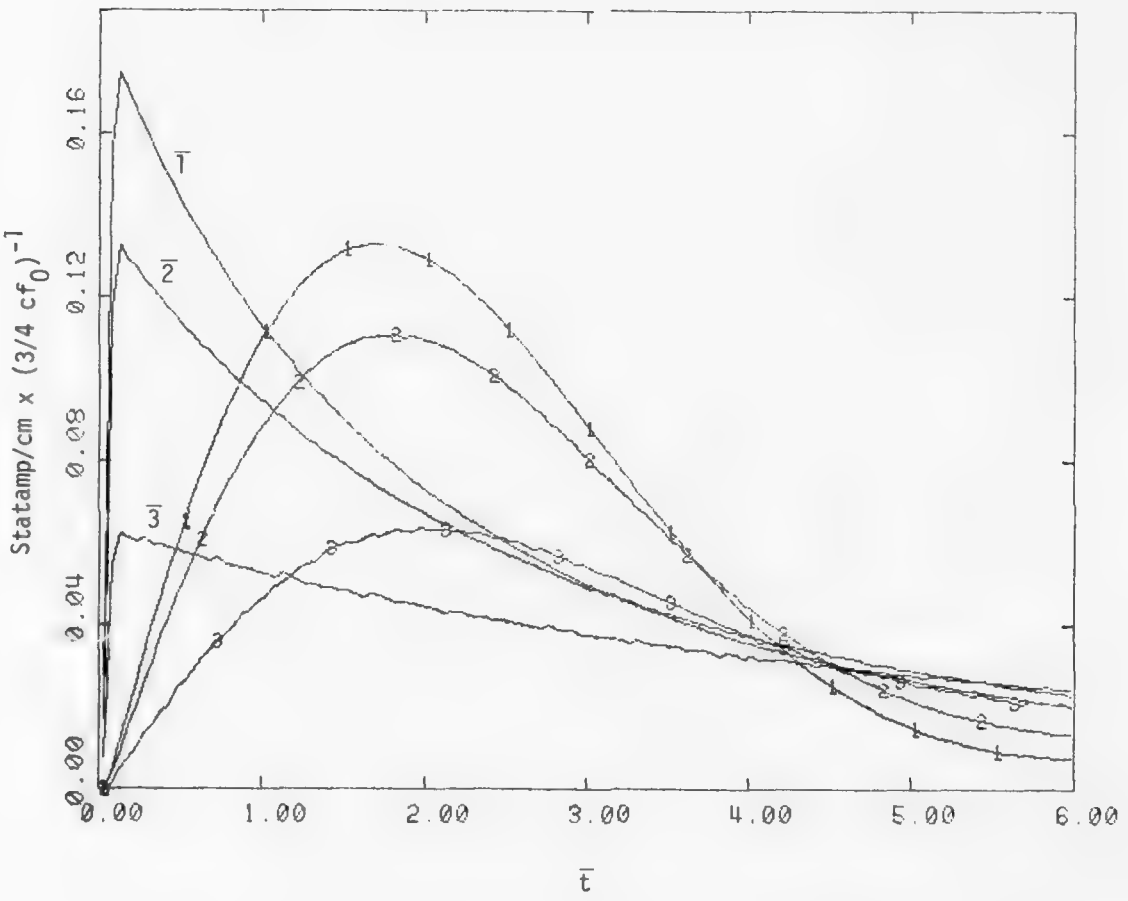

Figure 7. ℓ = 1, linear limit, triangular pulse excitation ($\bar{t}_f$ = .1). Skin current magnitude vs. normalized time.

$\bar{1}$ = quasi-static limit, v/c = .186; 1 = complete solution, v/c = .186

$\bar{2}$ = quasi-static limit, v/c = .136; 2 = complete solution, v/c = .136

$\bar{3}$ = quasi-static limit, v/c = .063; 3 = complete solution, v/c = .063

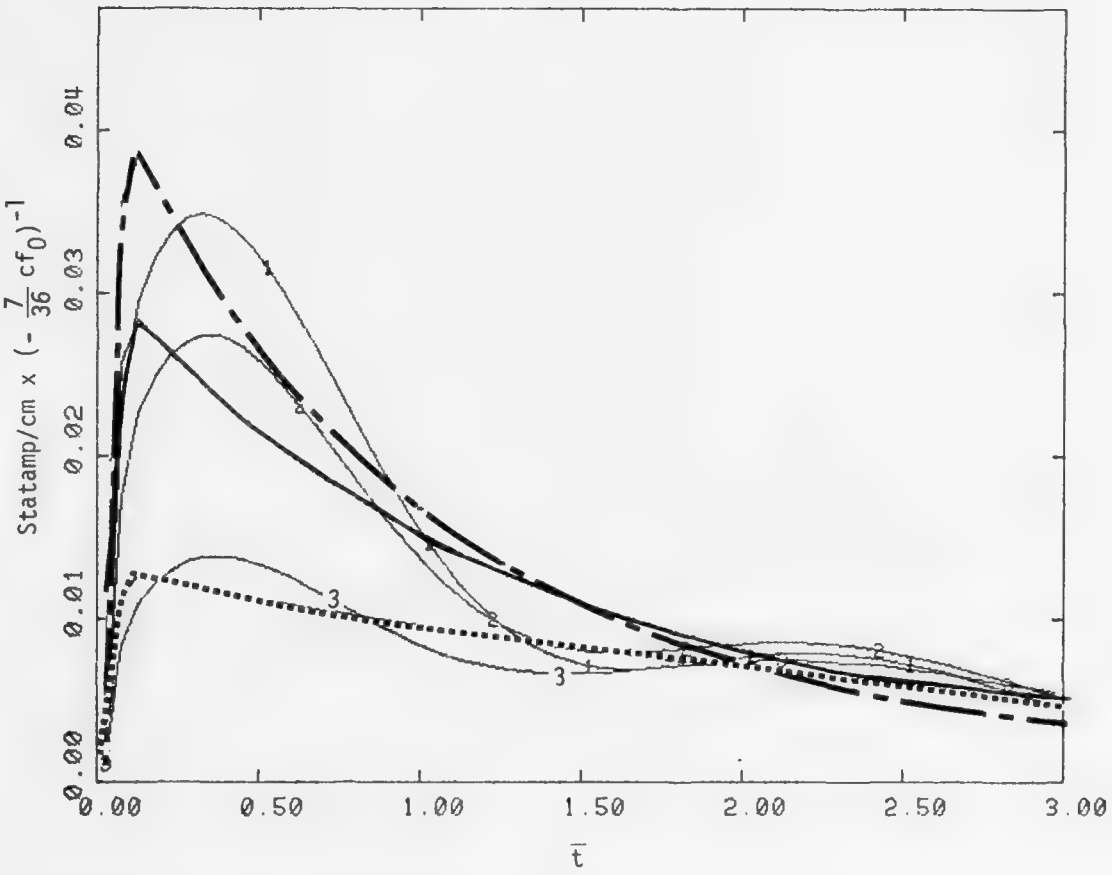

Figure 8. ℓ = 3, linear limit, triangular pulse excitation ($\bar{t}_f$ = .1). Skin current magnitude vs. normalized time.

——— quasi-static limit, v/c = .186; 1 = complete solution, v/c = .186

——— quasi-static limit, v/c = .136; 2 = complete solution, v/c = .136

····· quasi-static limit, v/c = .063; 3 = complete solution, v/c = .063

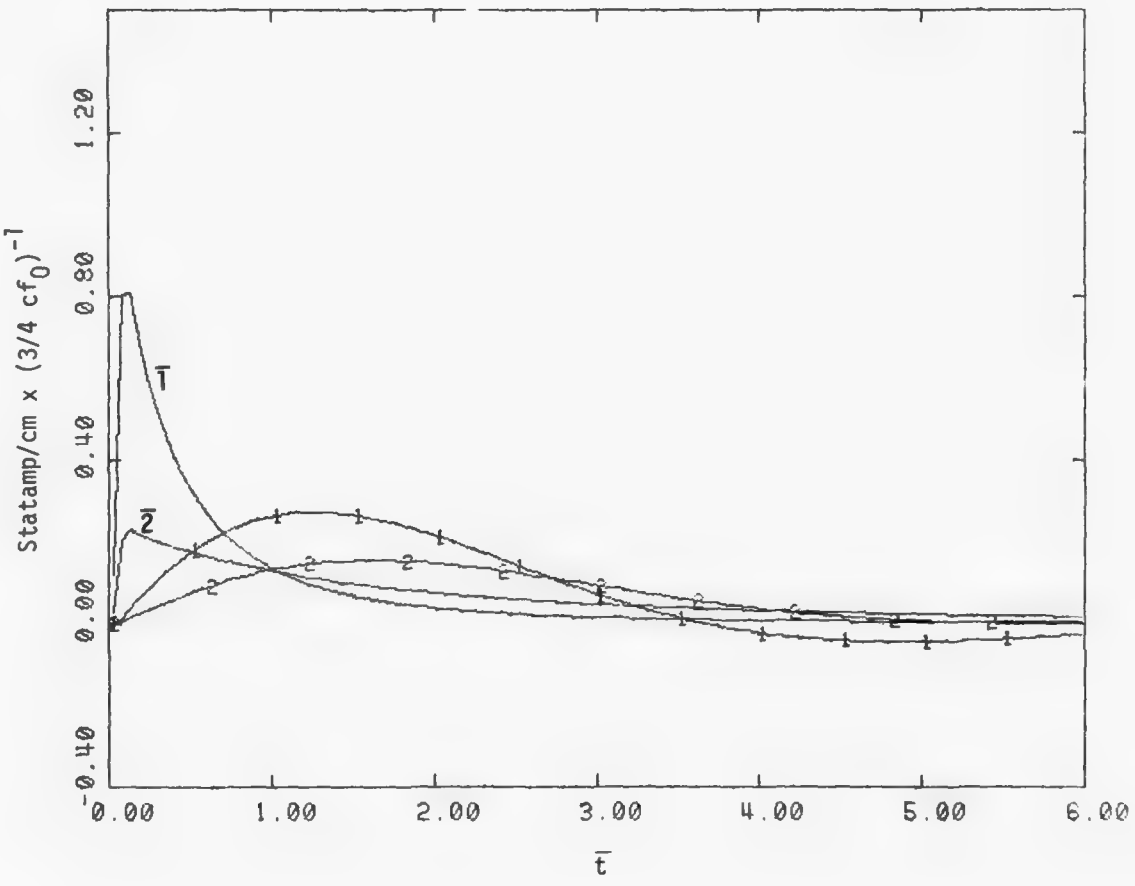

Figure 9. ℓ = 1, linear limit, triangular pulse excitation ($\bar{t}_f$ = .1). Skin current magnitude vs. normalized time.

$\bar{1}$ = quasi-static limit, v/c = 1; 1 = complete solution, v/c = 1

$\bar{2}$ = quasi-static limit, v/c = .239; 2 = complete solution, v/c = .239

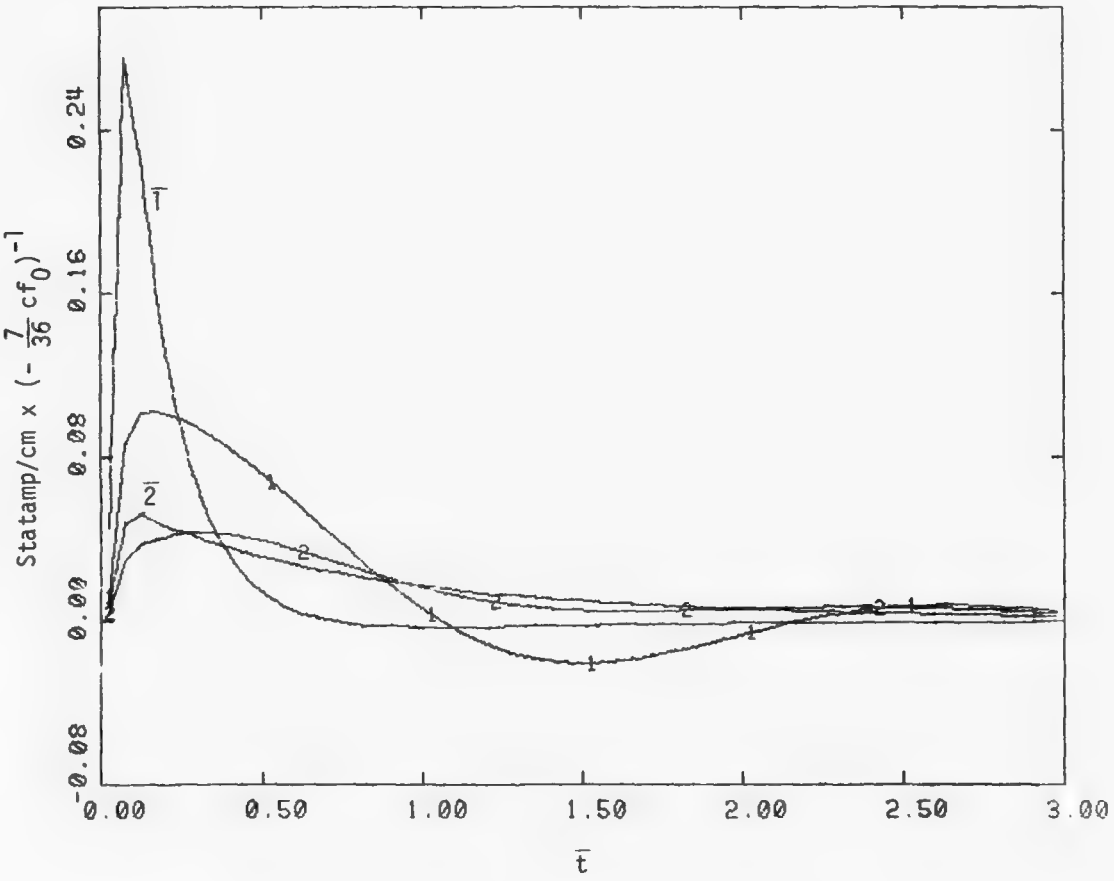

Figure 10. $\ell = 3$, linear limit, triangular pulse excitation ($\bar{t}_f = .1$). Skin current magnitude vs. normalized time.

$\bar{1}$ = quasi-static limit, v/c = 1; 1 = complete solution, v/c = 1

$\bar{2}$ = quasi-static limit, v/c = .239; 2 = complete solution, v/c = .239

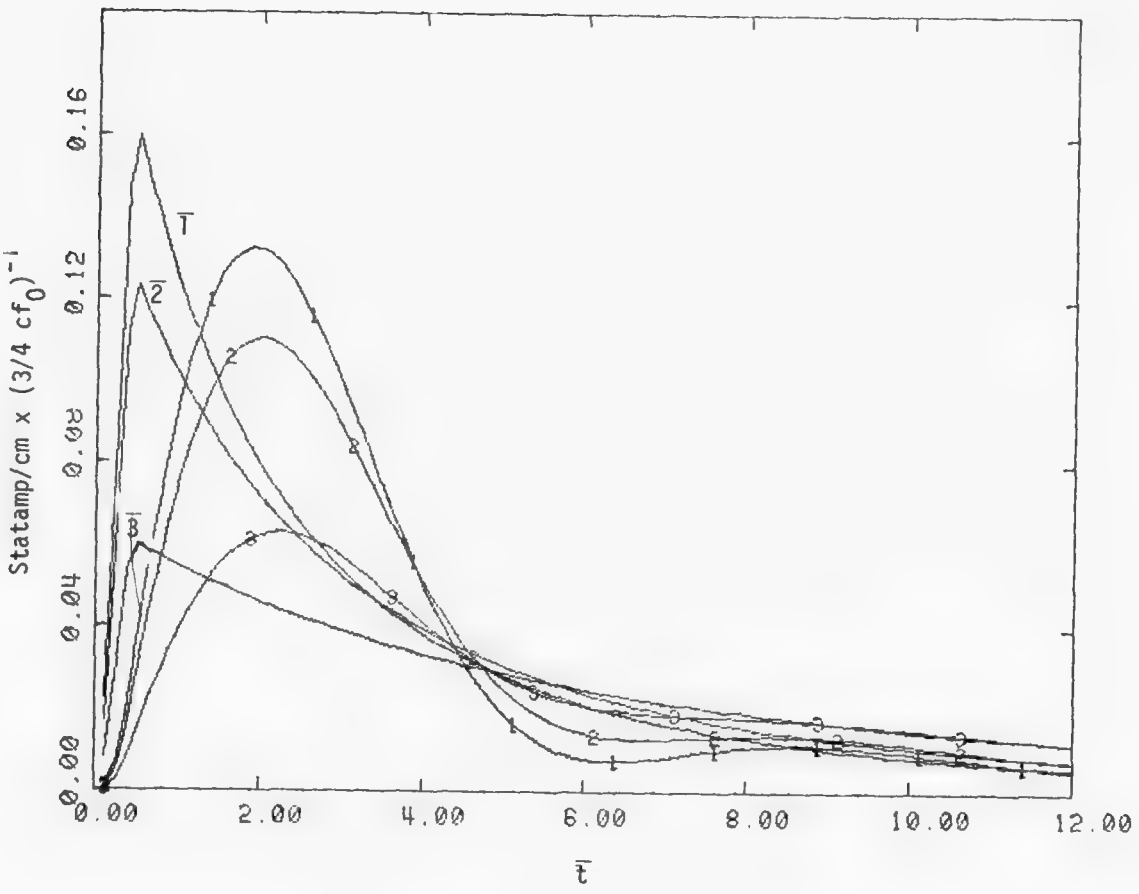

Figure 11. ℓ = 1, linear limit, triangular pulse excitation ($\bar{t}_f$ = .5). Skin current magnitude vs. normalized time.

$\bar{1}$ = quasi-static limit, v/c = .186; 1 = complete solution, v/c = .186

$\bar{2}$ = quasi-static limit, v/c = .136; 2 = complete solution, v/c = .136

$\bar{3}$ = quasi-static limit, v/c = .063; 3 = complete solution, v/c = .063

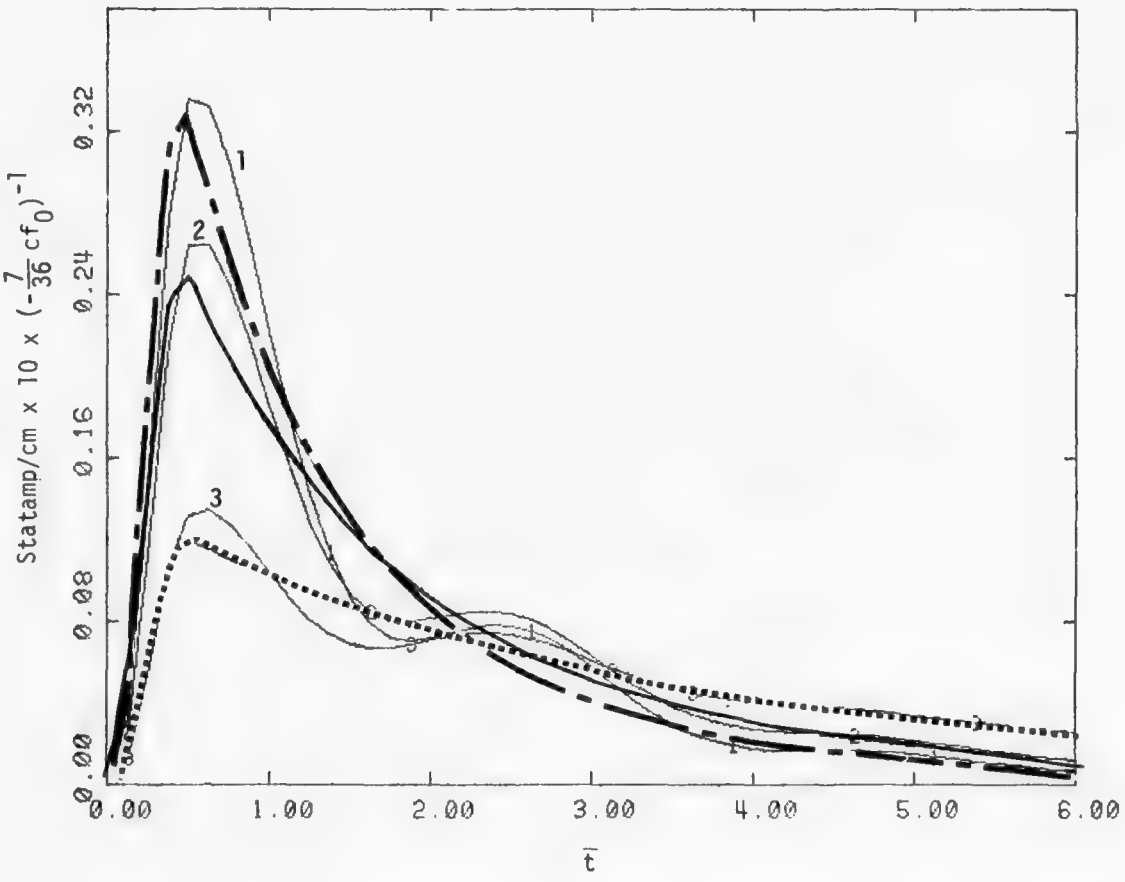

Figure 12. ℓ = 3, linear limit, triangular pulse excitation ($\bar{t}_f$ = .5). Skin current magnitude vs. normalized time.

— — — quasi-static limit, v/c = .186; 1 = complete solution, v/c = .186

——— quasi-static limit, v/c = .136; 2 = complete solution, v/c = .136

····· quasi-static limit, v/c = .063; 3 = complete solution, v/c = .063

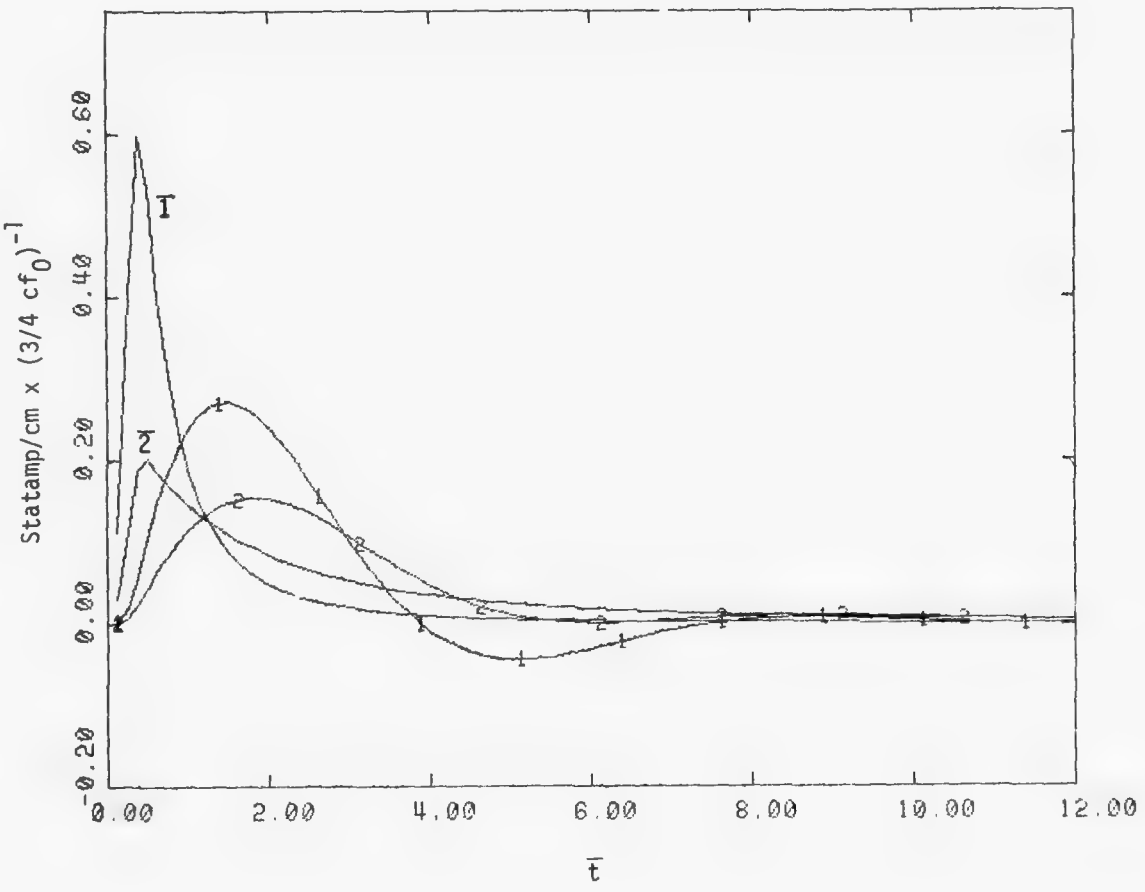

Figure 13. ℓ = 1, linear limit, triangular pulse excitation ($\bar{t}_f$ = .5). Skin current magnitude vs. normalized time.

$\bar{1}$ = quasi-static limit, v/c = 1; 1 = complete solution, v/c = 1

$\bar{2}$ = quasi-static limit, v/c = .239; 2 = complete solution, v/c = .239

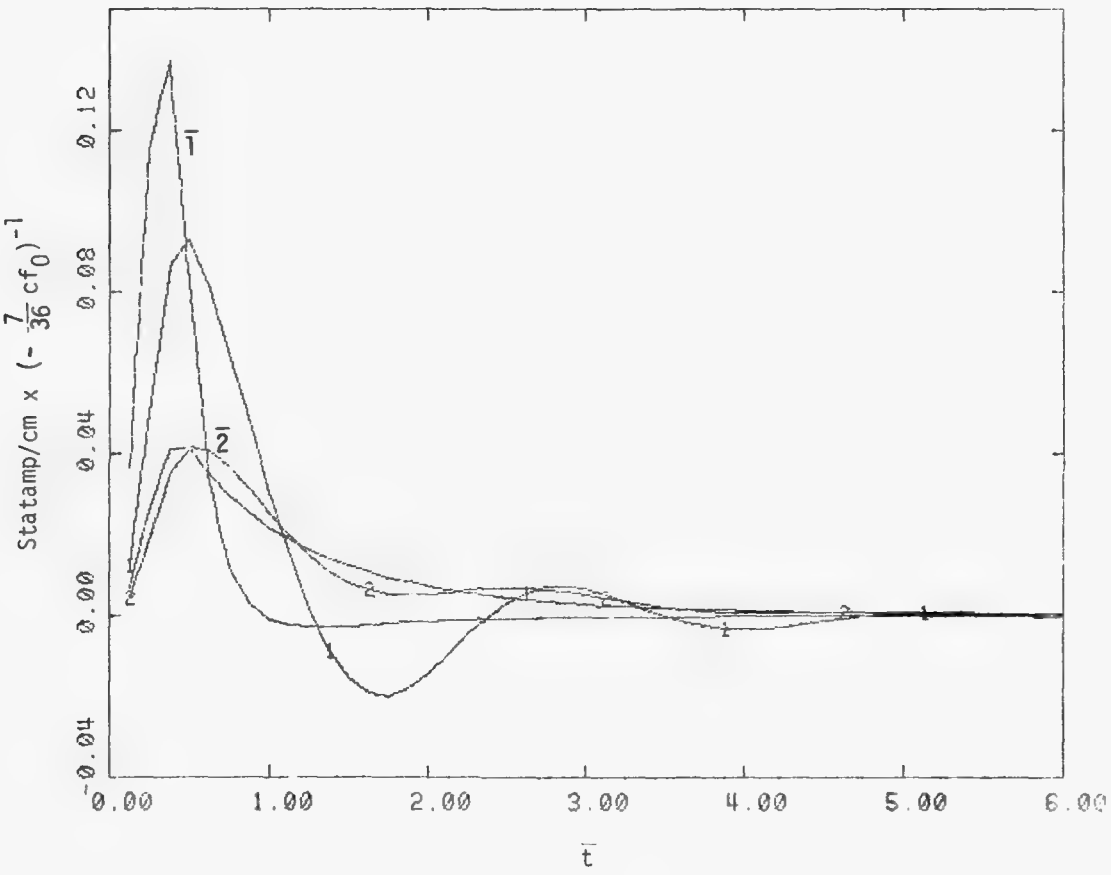

Figure 14. ℓ = 3, linear limit, triangular pulse excitation ($\bar{t}_f$ = .5). Skin current magnitude vs. normalized time.

$\bar{1}$ = quasi-static limit, v/c = 1; 1 = complete solution, v/c = 1

$\bar{2}$ = quasi-static limit, v/c = .239; 2 = complete solution, v/c = .239

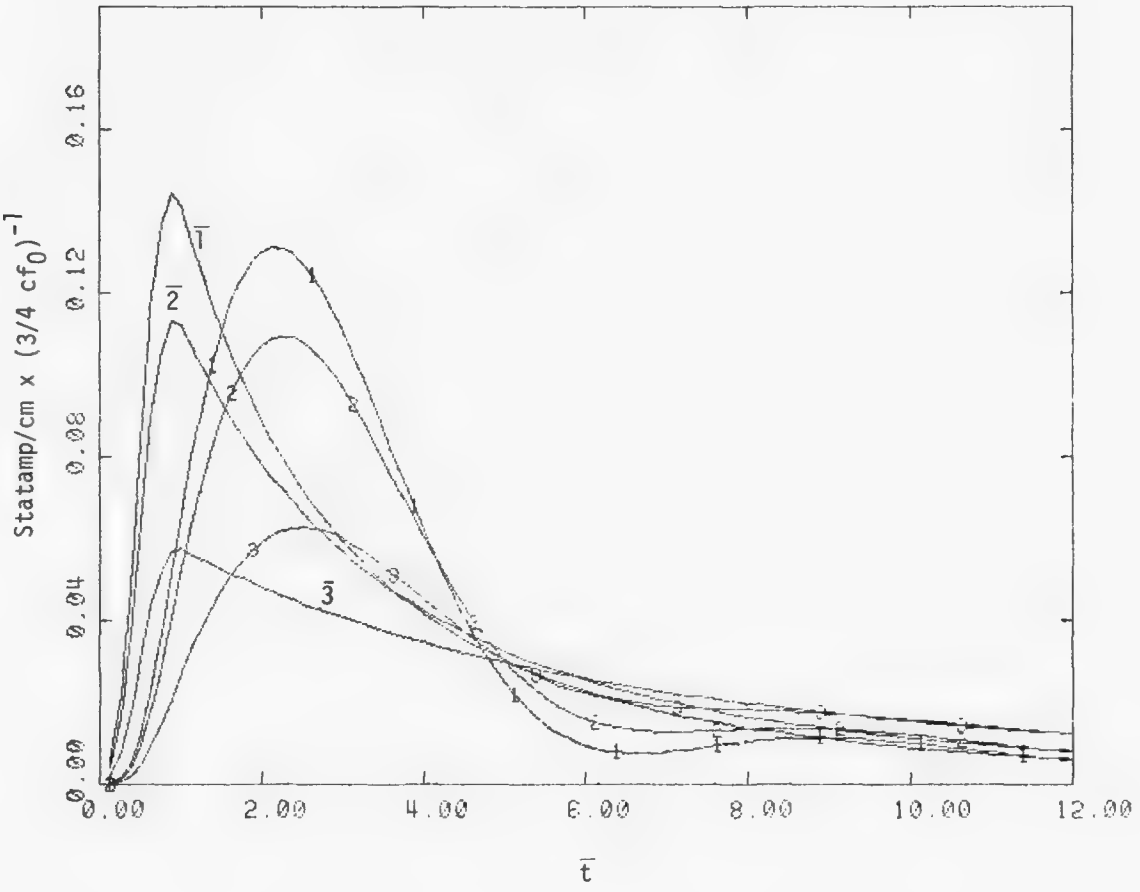

Figure 15. ℓ = 1, linear limit, triangular pulse excitation ($\bar{t}_f$ = 1.0). Skin current magnitude vs. normalized time.

$\bar{1}$ = quasi-static limit, v/c = .186; 1 = complete solution, v/c = .186

$\bar{2}$ = quasi-static limit, v/c = .136; 2 = complete solution, v/c = .136

$\bar{3}$ = quasi-static limit, v/c = .063; 3 = complete solution, v/c = .063

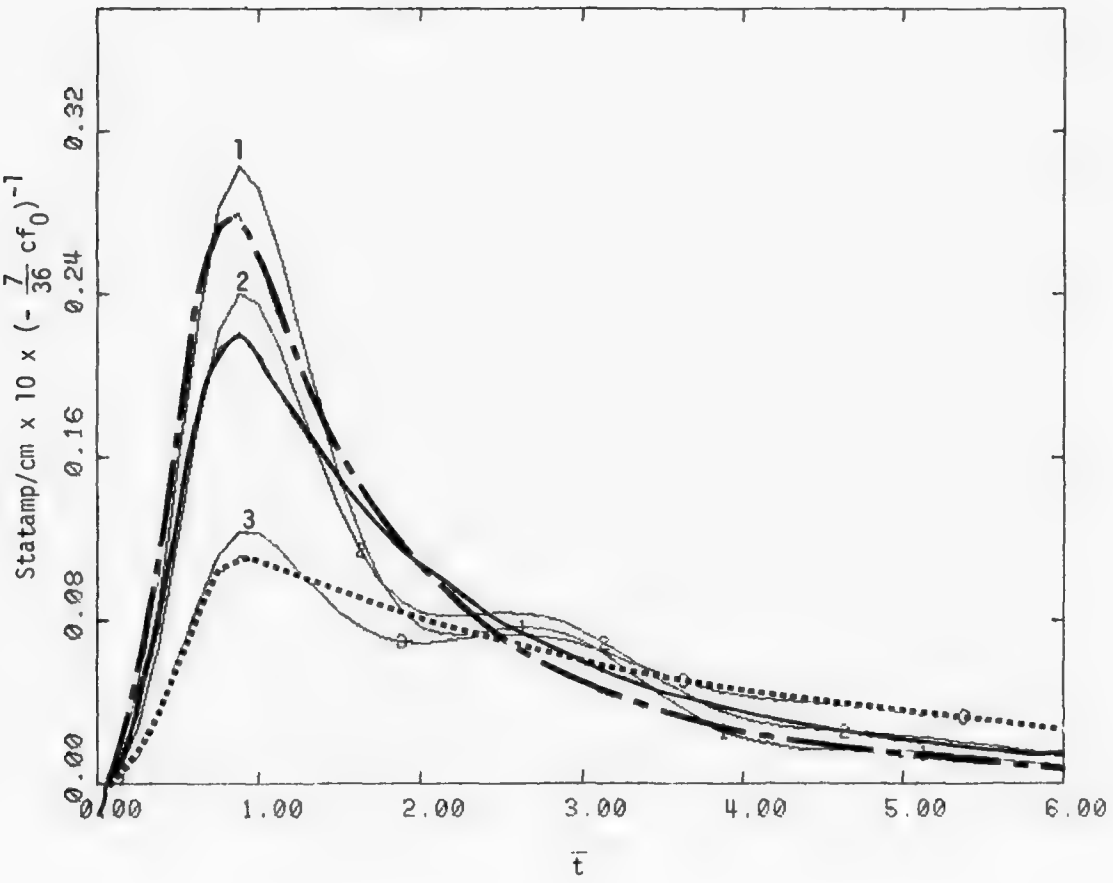

Figure 16. ℓ = 3, linear limit, triangular pulse excitation ($\bar{t}_f$ = 1.0). Skin current magnitude vs. normalized time.

——— – – – quasi-static limit, v/c = .186; 1 = complete solution, v/c = .186

——— quasi-static limit, v/c = .136; 2 - complete solution, v/c = .136

····· quasi-static limit, v/c = .063; 3 - complete solution, v/c = .063

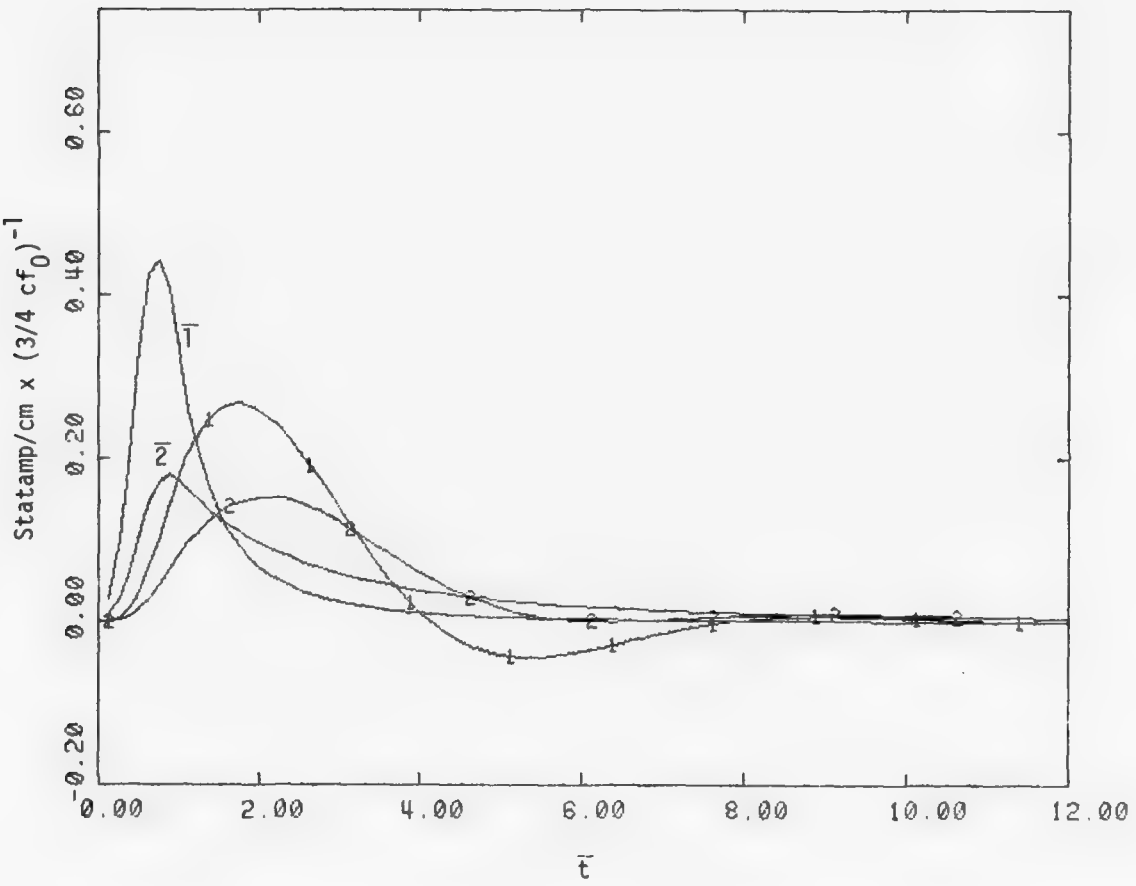

Figure 17. ℓ = 1, linear limit, triangular pulse excitation ($\bar{t}_f$ = 1.0). Skin current magnitude vs. normalized time.

$\bar{1}$ = quasi-static limit, v/c = 1; 1 = complete solution, v/c = 1

$\bar{2}$ = quasi-static limit, v/c = .239; 2 = complete solution, v/c = .239

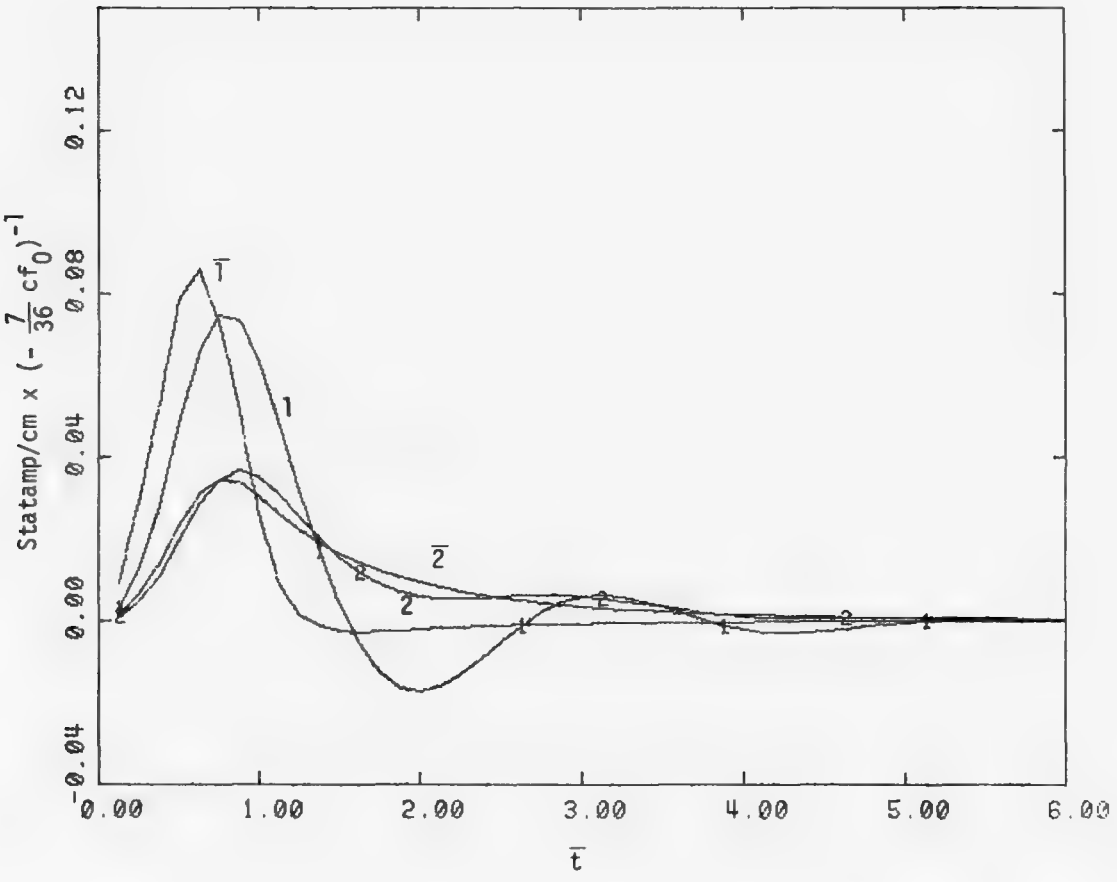

Figure 18. ℓ = 3, linear limit, triangular pulse excitation ($\bar{t}_f$ = 1.0). Skin current magnitude vs. normalized time.

$\bar{1}$ = quasi-static limit, v/c = 1; 1 = complete solution, v/c = 1

$\bar{2}$ = quasi-static limit, v/c = .239; 2 = complete solution, v/c = .239

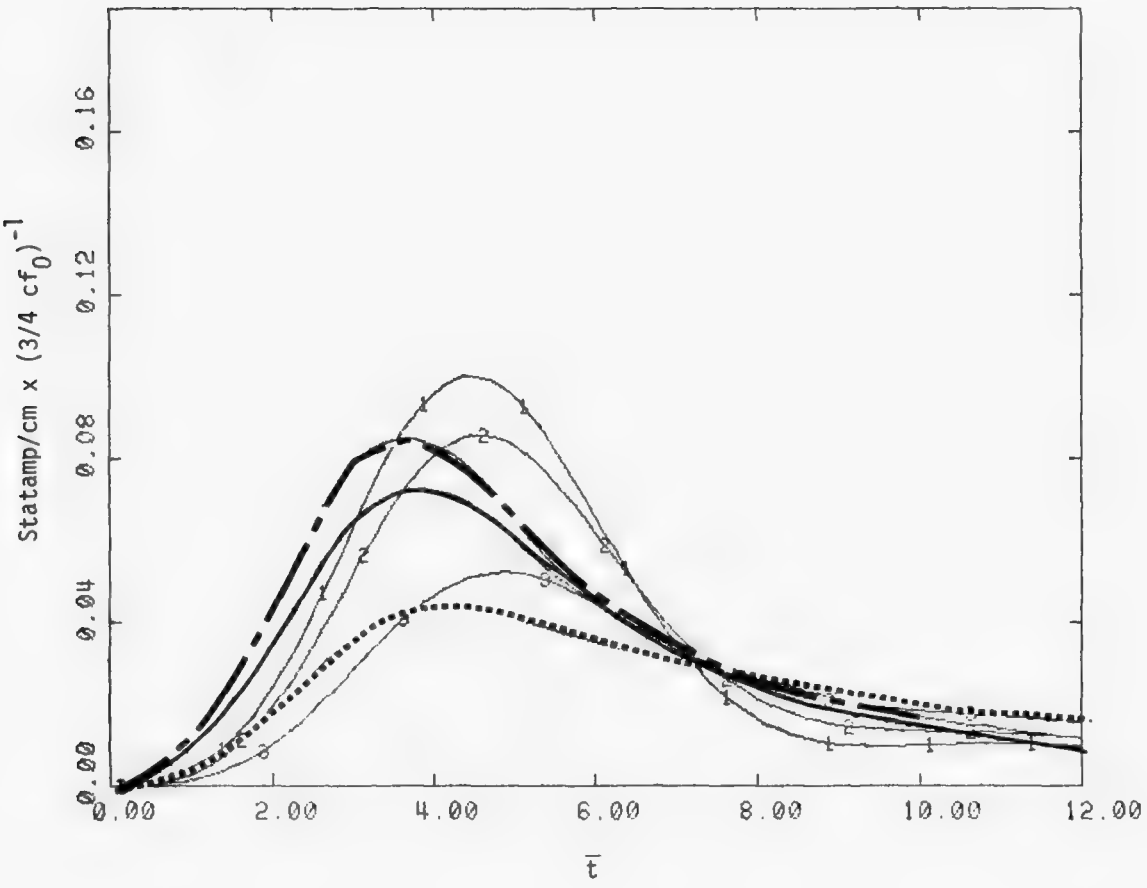

Figure 19. ℓ = 1, linear limit, triangular pulse excitation ($\bar{t}_f$ = 5.0). Skin current magnitude vs. normalized time.

——— quasi-static limit, v/c = .186; 1 = complete solution, v/c = .186

——— quasi-static limit, v/c = .136; 2 = complete solution, v/c = .136

..... quasi-static limit, v/c = .063; 3 = complete solution, v/c = .063

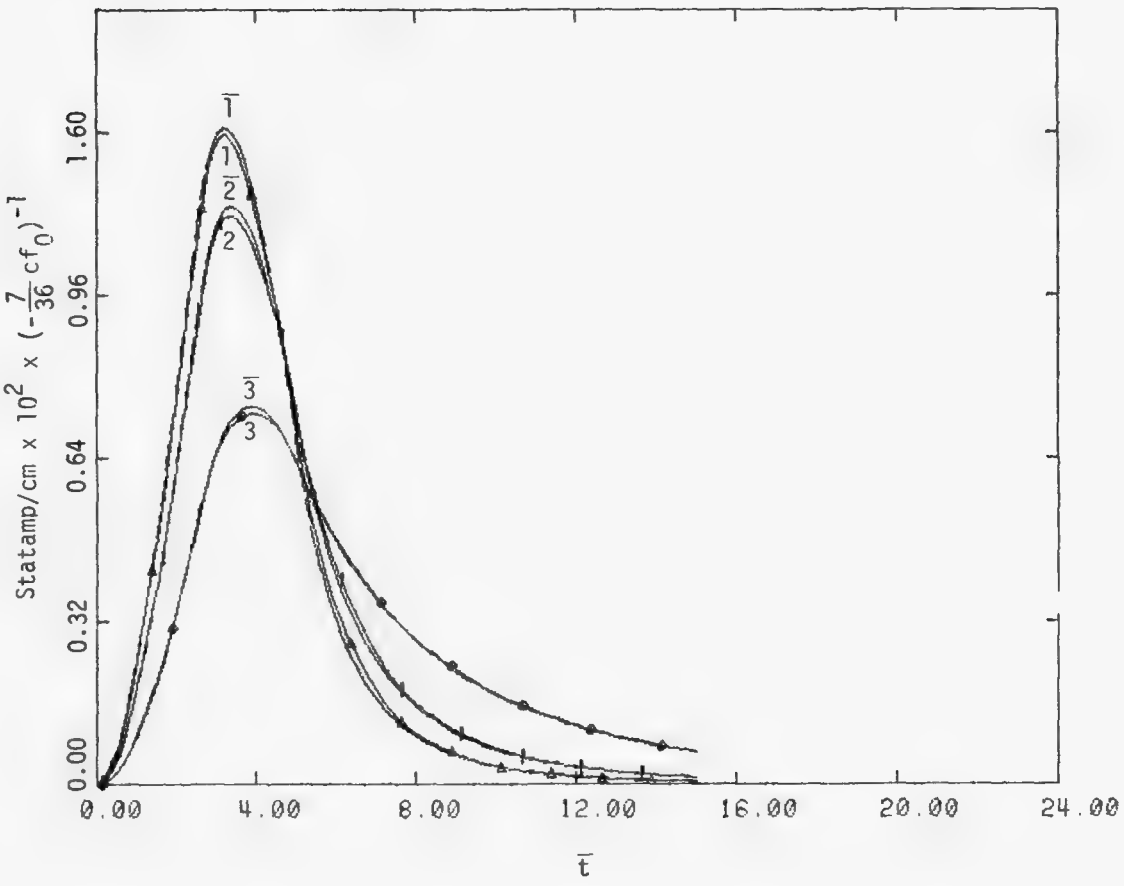

Figure 20. ℓ = 3, linear limit, triangular pulse excitation ($\bar{t}_f$ = 5.0). Skin current magnitude vs. normalized time.

$\bar{1}$ = quasi-static limit, v/c = .186; 1 - complete solution, v/c = .186

$\bar{2}$ = quasi-static limit, v/c = .136; 2 = complete solution, v/c = .136

$\bar{3}$ = quasi-static limit, v/c = .063; 3 - complete solution, v/c = .063

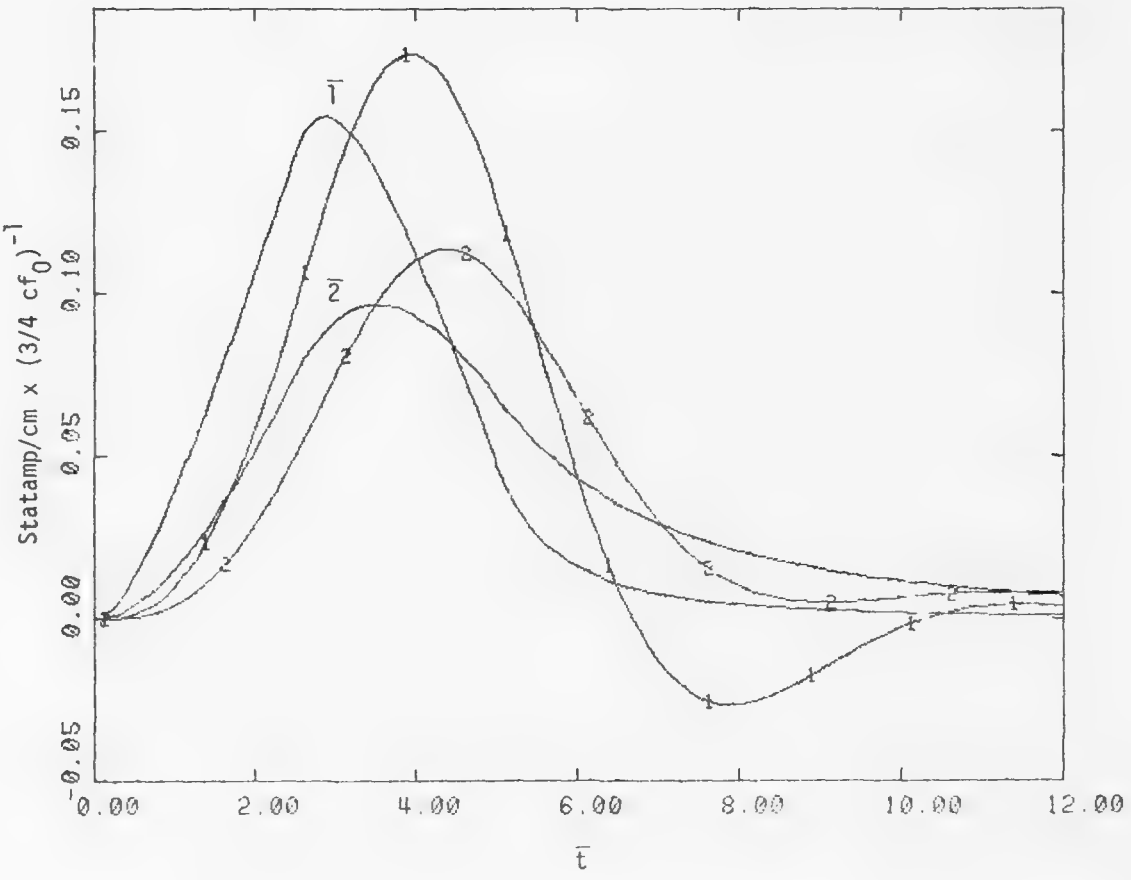

Figure 21. ℓ = 1, linear limit, triangular pulse excitation ($\bar{t}_f$ = 5.0). Skin current magnitude vs. normalized time.

$\bar{1}$ = quasi-static limit, v/c = 1; 1 = complete solution, v/c = 1

$\bar{2}$ = quasi-static limit, v/c = .239; 2 = complete solution, v/c = .239

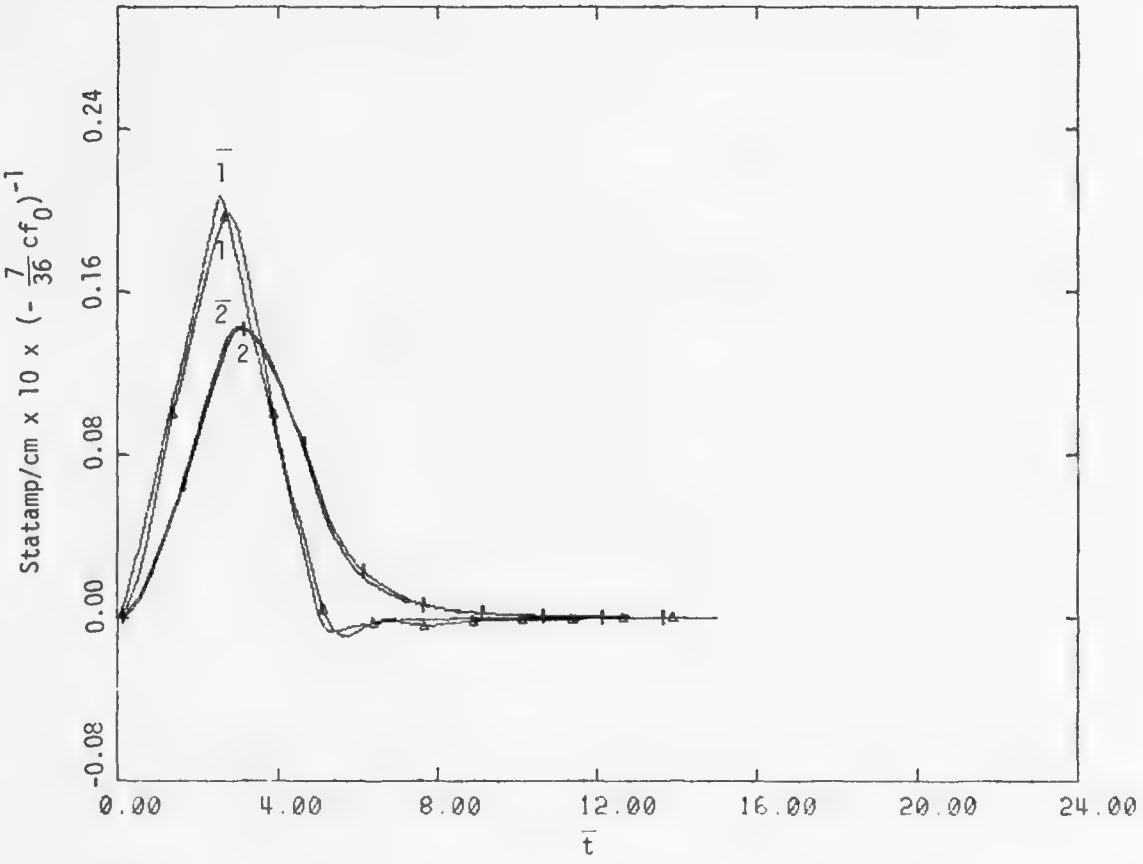

Figure 22. ℓ = 3, linear limit, triangular pulse excitation ($\bar{t}_f$ = 5.0). Skin current magnitude vs. normalized time.

$\bar{1}$ = quasi-static limit, v/c = 1; 1 = complete solution, v/c = 1

$\bar{2}$ = quasi-static limit, v/c = .239; 2 = complete solution, v/c = .239

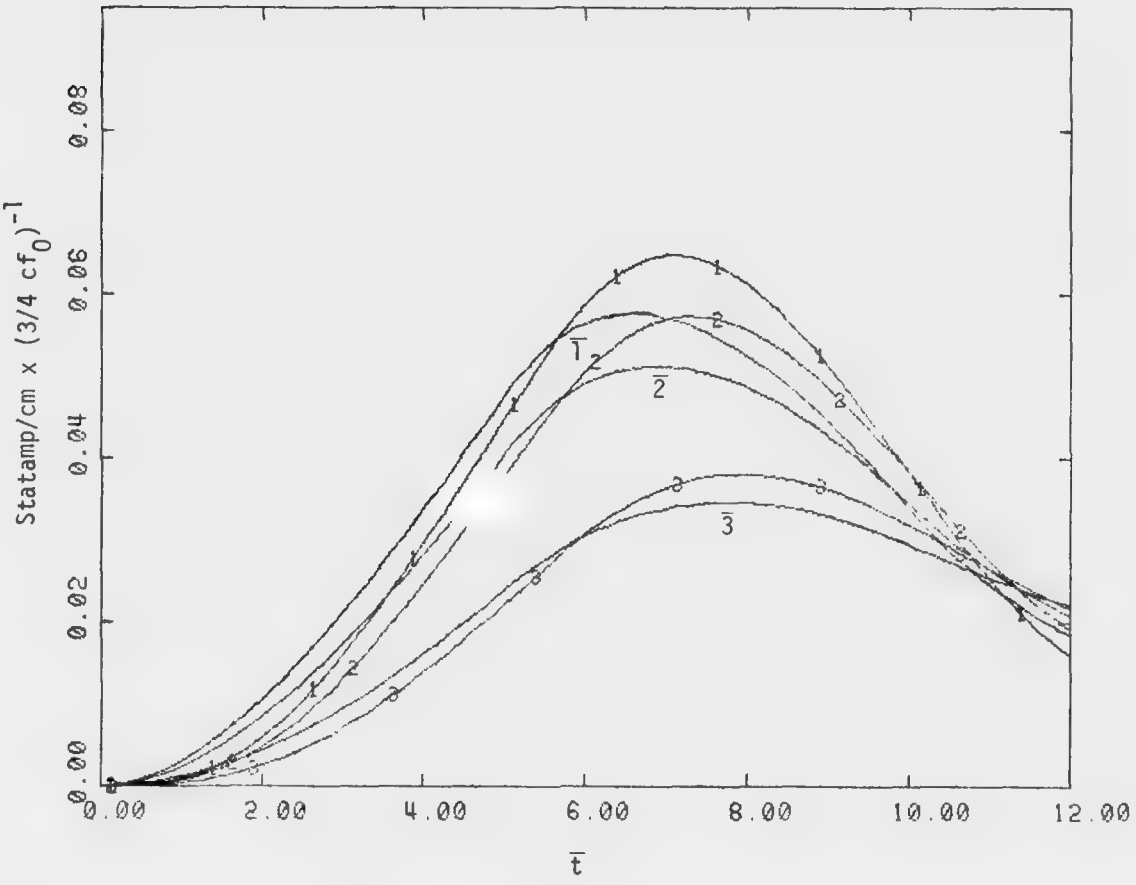

Figure 23. ℓ = 1, linear limit, triangular pulse excitation ($\bar{t}_f$ = 10). Skin current magnitude vs. normalized time.

$\bar{1}$ = quasi-static limit, v/c = .186; 1 = complete solution, v/c = .186

$\bar{2}$ = quasi-static limit, v/c = .136; 2 = complete solution, v/c = .136

$\bar{3}$ = quasi-static limit, v/c = .063; 3 = complete solution, v/c = .063

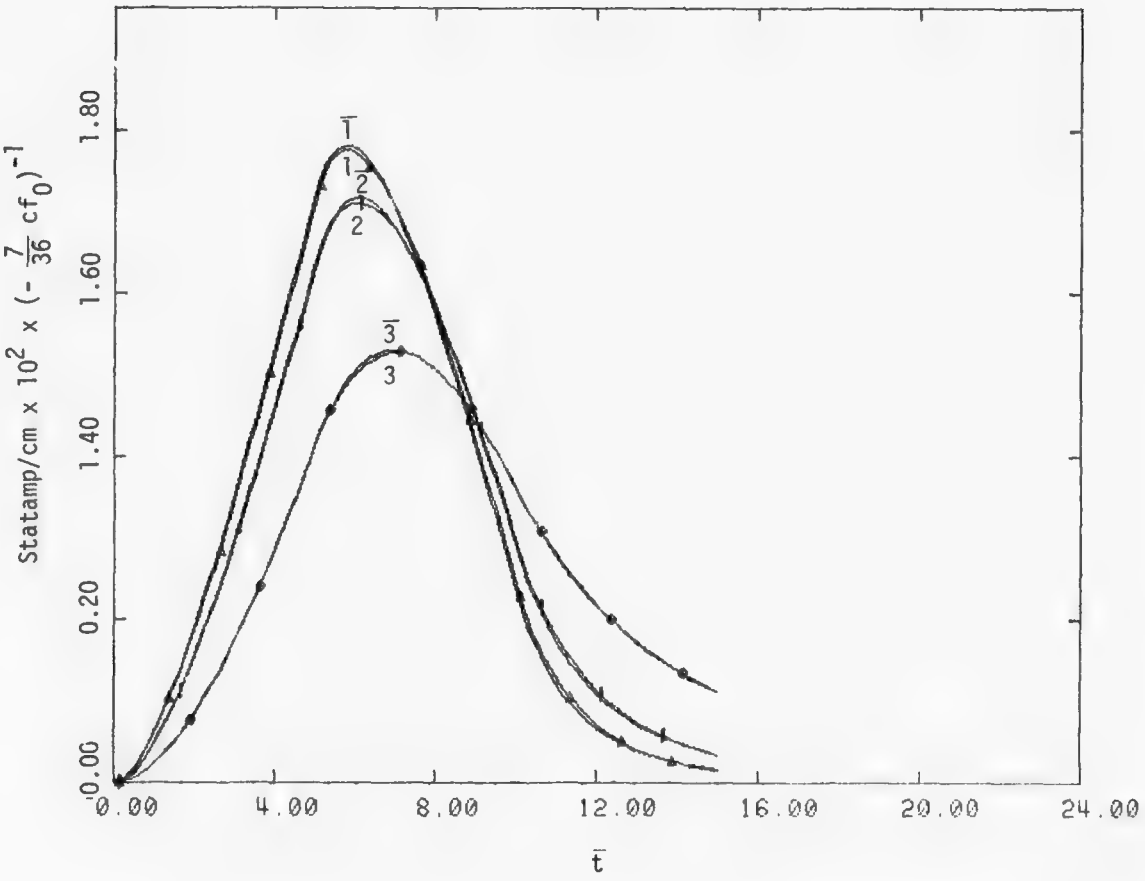

Figure 24. ℓ = 3, linear limit, triangular pulse excitation ($\bar{t}_f$ = 10). Skin current magnitude vs. normalized time.

$\bar{1}$ = quasi-static limit, v/c = .186; 1 = complete solution, v/c = .186

$\bar{2}$ = quasi-static limit, v/c = .136; 2 = complete solution, v/c = .136

$\bar{3}$ = quasi-static limit, v/c = .063; 3 = complete solution, v/c = .063

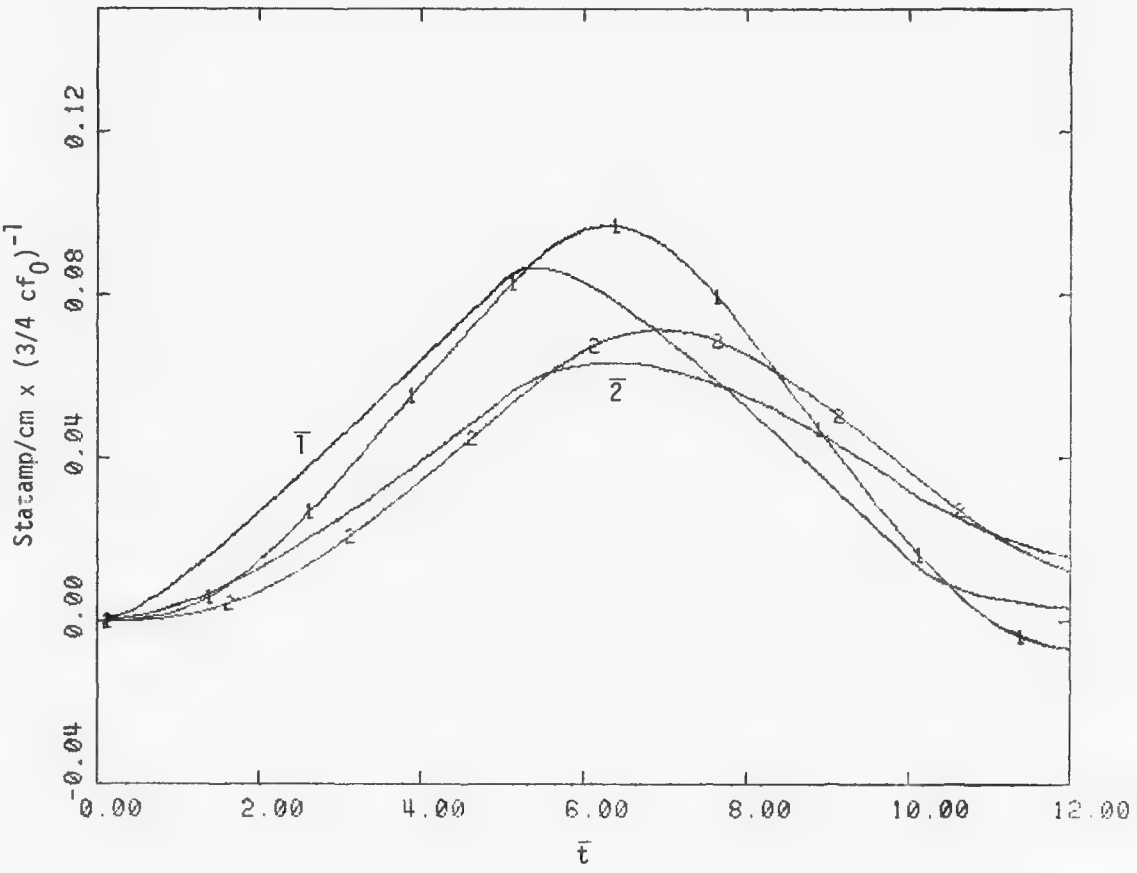

Figure 25. ℓ = 1, linear limit, triangular pulse excitation ($\bar{t}_f$ = 10). Skin current magnitude vs. normalized time.

$\bar{1}$ = quasi-static limit, v/c = 1; 1 = complete solution, v/c = 1

$\bar{2}$ = quasi-static limit, v/c = .239; 2 = complete solution, v/c = .239

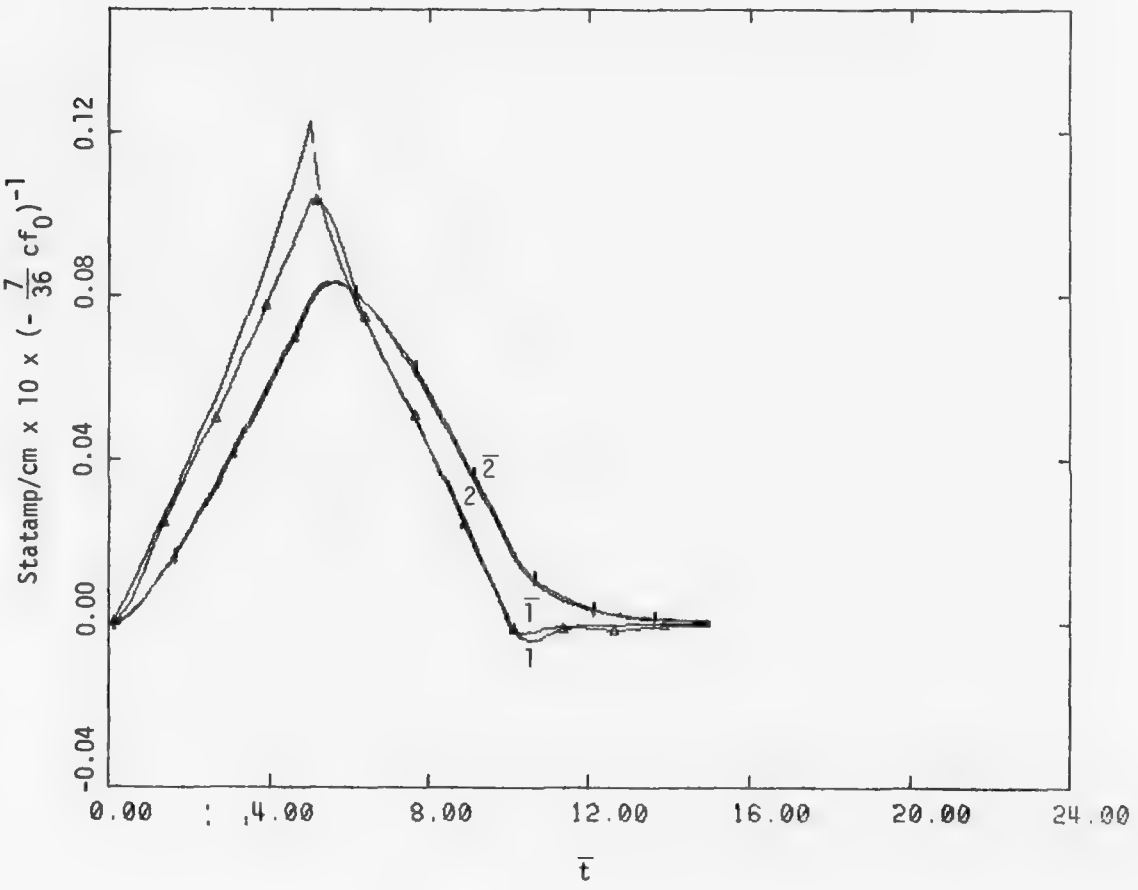

Figure 26. ℓ = 3, linear limit, triangular pulse excitation ($\bar{t}_f$ = 10). Skin current magnitude vs. normalized time.

$\bar{1}$ = quasi-static limit, v/c = 1; 1 = complete solution, v/c = 1

$\bar{2}$ = quasi-static limit, v/c = .239; 2 = complete solution, v/c = .239

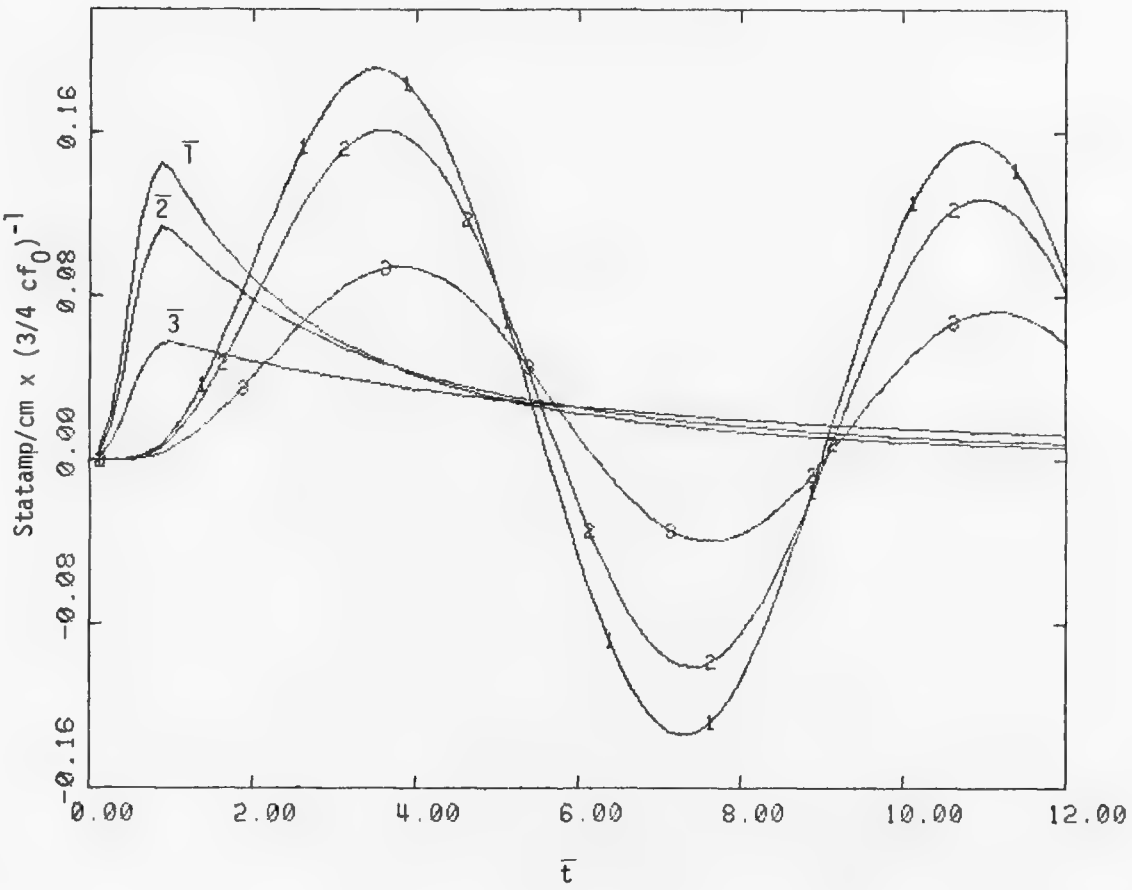

Figure 27. ℓ = 1, linear limit, triangular pulse excitation ($\bar{t}_f$ = 1.0). Skin current magnitude vs. normalized time. No damping.

$\bar{1}$ = quasi-static limit, v/c = .186; 1 = complete solution, v/c = .186

$\bar{2}$ = quasi-static limit, v/c = .136; 2 = complete solution, v/c = .136

$\bar{3}$ = quasi-static limit, v/c = .063; 3 = complete solution, v/c = .063

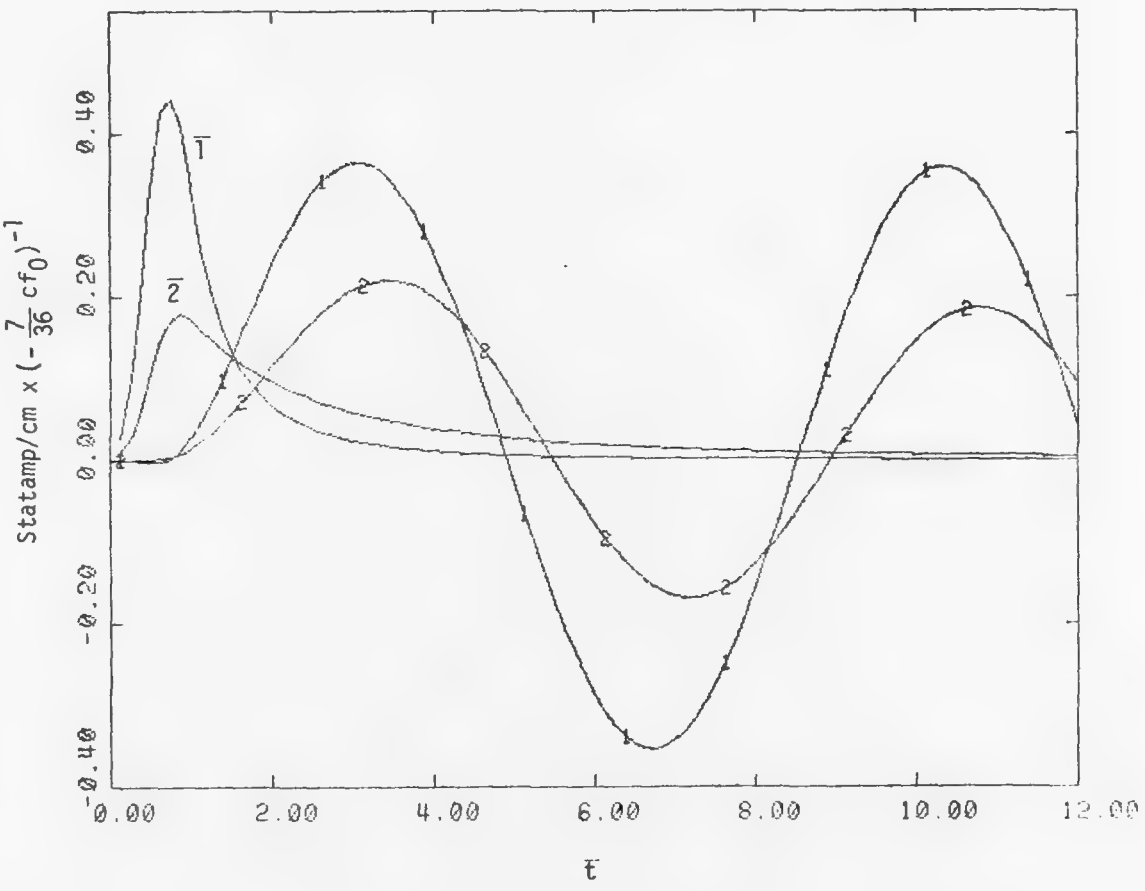

Figure 28. ℓ = 1, linear limit, triangular pulse excitation ($\bar{t}_f$ = 1.0). Skin current magnitude vs. normalized time.

$\bar{1}$ = quasi-static limit, v/c = 1; 1 = complete solution, v/c = 1

$\bar{2}$ = quasi-static limit, v/c = .239; 2 = complete solution, v/c = .239

current values for Figures 27 and 28 were made in the same way as those of Figures 7 through 26 except that $\overline{\sigma}_j^{\ell}$ was set equal to zero in Equation 71'. These latter two figures are made for $\overline{t}_f = 1$ only. Table 1 is a summary of two aspects of the total information contained in Figures 7 through 26. The maximum values of the skin current magnitudes (divided by $\frac{3}{4} cf_0$) are given along with the rise time (in units of t/τ) to attain this maximum value. The corresponding quasi-static values are given for comparison.

An example of how one might use Table 1 is the following. Suppose 2×10^{10} electrons/cm^2 leave a sphere of radius 3 meters in 10×10^{-8} seconds. We have, noting that 3×10^{10} cm/sec is the velocity of light.

$$\tau = \frac{300}{3 \times 10^{10}} = 10^{-8} \text{ sec} ,$$

$$\overline{t}_f = \frac{10 \times 10^{-8}}{10^{-8}} = 10 .$$

If we are convinced that most of the escaping electrons have a v/c value of .136 then looking at the table for a pulse length of 10 we find under "complete solution" a rise time of 7.25 and a maximum normalized skin current of 5.73×10^{-2}. The actual rise time then is

$$\tau(7.25) = 7.25 \times 10^{-8} \text{ sec} .$$

The actual skin current is

$$\frac{3}{4} cf_0(5.73 \times 10^{-2}) = (.75)(3 \times 10^{10})(2 \times 10^{10} \times 4.8 \times 10^{-10})(5.73 \times 10^{-2})$$

$$= 1.25 \times 10^{10} \frac{\text{statamp}}{\text{cm}} ,$$

4.8×10^{-10} is the charge of an electron. (To convert to amps/m we multiply by $.3 \times 10^{-7}$. For most all problems in the linear limit which require only the rise time and the maximum skin current, the $\ell = 1$ solution is a good approximation. The table is convenient for those problems which require a linear interpolation between table values.

Table 1. Linear limit maximum normalized skin currents and rise times.

v/c	Complete Solution		Quasi Static Sol	
	Maximum	Rise Time	Maximum	Rise Time
	t_f = Pulse Length = 10			
.063	3.81×10^{-2}	7.88	3.46×10^{-2} (9.2)	7.75 (1.6)
.136	5.73×10^{-2}	7.25	5.12×10^{-2} (10.6)	6.88 (5.1)
.186	6.47×10^{-2}	7.00	5.76×10^{-2} (10.9)	6.63 (5.3)
.239	7.14×10^{-2}	6.99	6.34×10^{-2} (11.2)	6.38 (7)
1.0	9.68×10^{-2}	6.25	8.67×10^{-2} (10.4)	5.38 (14)
	t_f = Pulse Length = 5			
.063	5.23×10^{-2}	4.88	4.40×10^{-2} (16)	4.25 (13)
.136	8.57×10^{-2}	4.63	7.23×10^{-2} (16)	3.87 (16)
.186	9.91×10^{-2}	4.25	8.47×10^{-2} (15)	3.63 (15)
.239	1.14×10^{-1}	4.38	9.67×10^{-2} (15)	3.5 (20)
1.0	1.74×10^{-1}	3.89	1.54×10^{-1} (11.3)	2.89 (25)
	t_f = Pulse Length = 1			
.063	5.27×10^{-2}	2.5	5.75×10^{-2} (-9.1)	1.00 (60)
.136	1.09×10^{-1}	2.25	1.13×10^{-1} (-3.7)	.875 (61)
.186	1.31×10^{-1}	2.13	1.45×10^{-1} (-10.7)	.875 (59)
.239	1.53×10^{-1}	2.13	1.79×10^{-1} (-17)	.875 (59)
1.0	2.69×10^{-1}	1.75	4.43×10^{-1} (-65)	.75 (57)
	t_f = Pulse Length = .5			
.063	6.31×10^{-2}	2.3	6.0×10^{-2} (5)	.5 (80)
.136	1.10×10^{-1}	2.0	1.2×10^{-1} (-9)	.5 (75)
.186	1.32×10^{-1}	1.9	1.6×10^{-1} (-23)	.5 (74)
.239	1.55×10^{-1}	1.9	2.0×10^{-1} (-25)	.5 (74)
1.0	2.72×10^{-1}	1.5	6.0×10^{-1} (-120)	.4 (73)

SECTION 5

DISCUSSION

In this section the results presented in the previous section will be discussed. To aid in understanding the results, reference will continually be made to the quasi-static limit. Apart from understanding the results, a point of view which we want to examine is to what extent the quasi-static limit can be used as an approximation to the actual skin current. Put in another way, we would like to judge how much of the sphere response (the number of modes) need we treat in a fully time-dependent manner and how much of the response can we legitimately approximate quasi-statically. For systems which are not as highly damped as the conducting sphere, we would also like to gain some insight into the validity of this viewpoint.

The quasi-static or low-frequency limit, for the skin current on a sphere, was derived in Reference 1 by taking the limiting form of the Green's Function (the same effect could be achieved by letting $k \to 0$ in Equation 13). In our discussion of low- and high-frequency limits at the end of this section, we take the limits of the skin currents, which were obtained by using the exact Green's function. Looking at Figures 1 and 3 it appears that, for $\bar{t}_f > 10$, in the non-linear limit, the quasi-static limit will be a very reasonable approximation to the actual skin current response of the sphere. (For definiteness we will assume that the quasi-static solution is a good approximation when, for a given "ℓ," three conditions are satisfied: (1) the main peak of the quasi-static solution differs by less than 15 percent from the main peak of the fully time dependent solution, (2) the rise time to the peak of the quasi-static solution differs from the corresponding rise

time of the fully time-dependent solution by less than 15 percent and (3) the secondary peaks of the main solution are less than 15 percent of the peak of the quasi-static solution.) By examining Equations 68', 69' and 71' it is clear that the magnitude of the oscillatory responses (the terms that basically cause the time dependent solution to differ from the quasi-static limit) depends upon the damping constant $\bar{\sigma}_j^{\ell}$. Figure 2 demonstrates what happens if the damping is zero ($\bar{\sigma}_j^{\ell} = 0$) in the integral of Equation 71', for $\ell = 1$ and $t_f = 12$. The quasi-static solution would no longer meet our criteria for a good approximation. This latter argument should be taken as more intuitive than exact since the factors that multiply the oscillatory response terms depend upon the magnitude of $\bar{\sigma}_j^{\ell}$. Nonetheless it is probably correct to say that strong damping extends the validity of the quasi-static treatment. This is a particularly useful criteria for picking important modes of arbitrary structures. In determining whether or not a mode with period T will be excited by a pulse whose length is t_f one usually judges that if

$$T/t_f \sim 1 \ , \tag{87}$$

the mode will be strongly excited. For a system having a particular mode which damps with an e folding time of t_D the mode will not be as strongly excited if

$$t_f/t_D > \eta \ , \tag{88}$$

(η is a number characteristic of the mode), in spite of the satisfaction of Equation 87. In the sphere problem, for $1 < \bar{t}_f < 10$, treating the $\ell = 1$ mode in a fully time-dependent manner while treating the rest of the modes quasi-statically would result in a reasonable approximation for the skin current. For $\bar{t}_f \leq 1$, in Figure 1 the magnitude of the fully time-dependent response differs quite considerably in magnitude and time dependence from the quasi-static response. As $\bar{t}_f$ approaches zero, both the $\ell = 1$ and $\ell = 3$ (Figure 3) time-dependent responses approach zero. Investigation of modal response, for this example, in the pulse length range $\bar{t}_f < 1$ would require examination of higher modes.

The oscillatory portion of Equation 75' is contained in the term S^1_{12} which is defined in Equation 71'. Since S^1_{12} involves a second derivative, oscillations are stimulated when the slope of $\bar{f}(\bar{t})$ changes. The slope of the triangular time function defined by Equations 77 to 80 changes, discontinuously, at three points. Specifically for $\bar{t} < \bar{t}_f/2$, Equation 75 yields

$$K_1 = c\,\frac{3}{4}\,f_0\beta(\bar{t} + \frac{2}{\sqrt{3}}\,e^{-.5\bar{t}}\sin\sqrt{3}/2\,\bar{t}) \quad , \tag{89}$$

where use has been made of Equations 63. When the slope of $\bar{f}(\bar{t})$ changes continuously K_1 cannot be represented as simply as Equation 89. Figure 4 shows the effect on the skin current magnitudes when a smooth continuously changing $\bar{f}(\bar{t})$ is used. A comparison of Figures 4, 2 and 1 show that the effects on the $\ell = 1$ skin currents are much the same (relative to the quasi-static solution), with a given pulse length, for either the smooth or the discontinuous pulse. A number of things can be seen by inspecting the simple form of Equation 89. The oscillatory term begins from zero at $\bar{t} = 0$. As the sine term gets larger the amplitude drops due to the damping exponential. The sine term reaches its maximum at $\bar{T}/4$ ($\bar{T}$ is the normalized period of oscillation for $\ell = 1$) which is $\pi/\sqrt{3}$ for $\ell = 1$. At $\bar{t} = \bar{T}/4$ in Equation 89 the ratio of the oscillatory term to the quasi-static term ($\bar{t}$) is .25. If the damping term were not present the ratio of the two terms would be .64. This reasoning leads us to a more precise statement of Equations 87 and 88 for the $\ell = 1$ mode with a triangular pulse. The term $e^{-.5\bar{t}}\sin\sqrt{3}/2\,\bar{t}$ reaches its maximum of .47 at $\bar{t} = 1.2$, so that in order for the oscillatory term to be only 15 percent, say, of the maximum of the quasi-static term the expression

$$.15\,\bar{t}_f/2 > \frac{2}{\sqrt{3}}\,(.47) \quad , \tag{90}$$

must be satisfied. $\bar{t}_f$, then is determined by

$$\bar{t}_f > 7.2 \quad . \tag{91}$$

Since $\bar{t}_D = 2$, we have, in this case

$$\frac{t_f}{t_D} \cong 4 \ . \tag{92}$$

That is η in Equation 88 is roughly 4. Since the normalized period of oscillation is $4\pi/\sqrt{3}$, we also have

$$T/t_f \cong 1.0 \ . \tag{93}$$

The characteristics of Figures 5 and 6 are much like those of Figures 1 through 3 and so we proceed to a discussion of the linear limit and Figures 7 through 28. Table 1 summarizes some of the pertinent data contained in these graphs. The table shows the maximum normalized skin current rise time for the $\ell = 1$, complete time-dependent and quasi-static solutions. The numbers in the upper left hand corners of the table entries, appropriate to the quasi-static solution, are the percent difference between the complete solution and the quasi-static solution. For a pulse length $\bar{t}_f = 10$ both the rise time and the maximum are within 15 percent of each other for both solutions. When $\bar{t}_f = 5$ the rise times begin to differ by more than 15 percent when $v/c > .186$. A look at Figures 22 and 24 shows that the $\ell = 3$ quasi-static solution is a good approximation even when $v/c > .186$ at $\bar{t}_f = 5$. If $\bar{t}_f = 1$ the difference in rise times between the two solutions in Table 1 is roughly 60 percent. The magnitudes, however, are surprisingly close for $v/c \leq .239$.

Figures 27 and 28 are plots of skin current magnitude for $\bar{t}_f = 1$ where the damping has been set equal to zero in the integrals defined by Equation 71'. These curves are suggestive of the differences that would occur between the complete time-dependent solution and the quasi-static solution for a system whose modes aren't damped as strongly as those of the sphere. Large differences occur in the first peak and not just after the driving pulse is over.

If one were constructing a hybrid of quasi-static and time-dependent modal solutions for a problem, similar to the one being discussed,

a table, such as Table 1, for both the $\ell = 1$ and $\ell = 3$ modal responses would define the ranges of validity of the quasi-static solution. Practically speaking, it is doubtful that many problems, involving a conducting sphere, in the linear limit, would require more than one or two fully time-dependent modes for an accurate description, over most of the interesting time range.

LOW AND HIGH FREQUENCY LIMITS

In this portion of Section 4, starting with Equations 68' and 69' we will first derive the low-frequency limit. The low-frequency or quasi-static limit is mentioned throughout this section. Using Equations 68' and 69' again we outline the derivation the high-frequency limit in the final part of this section. The high-frequency limit is important for appreciating results in the non-linear limit for $\bar{t}_f < 1$. If we assume that

$$\bar{\sigma}_j^{\ell}\bar{t}_f >> 1, \tag{94}$$

in Equation 71 then Equation 68' becomes

$$K_1(t) = cf_0(\tfrac{3}{4}) \int \frac{dx}{x^2}\left(\frac{\bar{f}(y)}{x} + (1 - \frac{1}{x})\frac{\partial f(y)}{\partial \bar{t}}\right). \tag{95}$$

Analogously Equation 69' becomes

$$K_2(t) = - cf_0 \frac{7}{48} \int \frac{dx}{x^2}\left(\frac{\bar{f}(y)}{x} + (1 - \frac{1}{x})\frac{\partial \bar{f}(y)}{\partial t}\right)\frac{1}{x^2}. \tag{96}$$

If $t >> (r - R)c^{-1}$ (the velocity of light is assumed to approach infinity) we also have $\bar{t} >> (x - 1)$. If we also assume that $v/c << 1$ then we can expand $\bar{f}(y)$ about $\bar{t} - (x - 1)\gamma$ using the definition expressed by Equation 70. The expansion is

$$\bar{f}(y) = \bar{f}(\bar{t} - (x-1)\gamma^{-1}) - (x-1)\frac{\partial f}{\partial \bar{t}}(\bar{t} - (x-1)\gamma^{-1}) + \mathcal{O}((x-1)^2) \quad . \tag{97}$$

Substituting Equation 97 into Equations 95 and 96 we have

$$K_1(t) \cong cf_0(\tfrac{3}{4}) \int \frac{dx}{x^2} f(t - (x-1)\gamma^{-1}) \frac{1}{x} \quad , \tag{98}$$

$$K_2(t) \cong -cf_0(\tfrac{7}{48}) \int \frac{dx}{x^2} \bar{f}(\bar{t} - (x-1)\gamma^{-1}) \frac{1}{x^3} \tag{99}$$

Equations 98 and 99 are expressions of the low-frequency linear limit. By neglecting the velocity and assuming that the integrands in this latter expression are multiplied by $\delta(x-1)$ we get the non-linear limit:

$$K_1(t) \cong cf_0(\tfrac{3}{4})\bar{f}(\bar{t}) \quad , \tag{100}$$

$$K_2(t) \cong -cf_0(\tfrac{7}{48})\bar{f}(\bar{t}). \tag{101}$$

The high-frequency limit is found by assuming that

$$e^{\sigma_j^{\ell}(t'-t)} \cong 1 + \sigma_j^{\ell}(t'-t) \quad , \tag{102}$$

and that

$$\cos(\alpha_j^{\ell}(t'-t)) \cong 1 \quad , \qquad \sin(\alpha_j^{\ell}(t'-t)) \cong \alpha_j^{\ell}(t'-t) \quad , \tag{103}$$

in Equations 68' and 69'. The resulting equations are

$$K_1(t) \cong cf_0(\tfrac{3}{4}) \int (\frac{dx}{x^2})(-\frac{1}{x} + 1) f(\bar{t}) \quad , \tag{104}$$

and

$$K_2(t) \cong - cf_0\left(\frac{7}{48}\right)\int \left(\frac{dx}{x^2}\right) \frac{f(\bar{t})}{x^2} \left(1 - \frac{1}{x}\right) . \qquad (105)$$

The integrand in expressions (104) and (105) is zero at x = 1. The numbers in Equation 105 have five place accuracy.

SECTION 6

SUMMARY AND CONCLUSIONS

This report can, perhaps, be divided into four areas of endeavor. These areas include the systematizing of some mathematical operations, an attempt at ellucidating a physical process, the presentation of some useful data and the expression of opinions as to the general applicability of modal analysis in SGEMP.

In order to investigate the effect on surface currents of a variety of external, axially symmetric source conditions, a good deal of mathematical manipulations are necessary. The manipulations are required to make the transition from a formal solution to a usable formalism. The solution for the currents on the surface of a conducting sphere is developed for odd ℓ, where ℓ designates the order of the Legendre polynomial expansion functions. Although not explicitly given in the report, the solution for even ℓ proceeds along the same lines.

Data is presented, for the $\ell = 1$ and $\ell = 3$ modes, with two assumed types of spatial source current configurations and many different source current time histories. This data is presented in graphs and a table so that, under certain restrictions, some estimates can be made in practical situations. The restrictions pertain to the model of the source currents and how well an object, in practice, conforms to the geometry of a conducting sphere.

The data for the time-dependent $\ell = 1$ and $\ell = 3$ solutions is compared with the low-frequency or quasi-static solution. Comparisons are made because, in general, quasi-static solutions are simple to obtain and

below a certain excitation frequency range they are a very good approximation to the whole true solution. The true time-dependent solution for these types of source current configurations—at least—is found to be, basically, the sum of the quasi-static solution plus oscillatory terms. The oscillatory terms are time integrals containing the damping and oscillatory frequencies of the spherical modes. Because of the high damping of the spherical modes, the oscillatory terms contribute less than might be expected so that the quasi-static solution is a valid estimate for a large range of source time histories. The treatment of the sphere then, in most situations encountered in practice, would probably not warrant more than the utilization of one or possibly two modes in a fully time-dependent manner. The other modes ($\ell > 3$, say) could be treated quasi-statically, if it was deemed necessary to use them.

The situation with the sphere suggests that the fields at the surface of more complicated objects could possibly be treated by a hybrid analysis of a few complete time-dependent modal contributions plus a quasi-static remainder. Criteria for choosing the modes to treat in a completely time-dependent manner, would depend on damping rate as well as their frequency of oscillation. Generally speaking, highly damped modes would contribute to the quasi-static remainder only. The integrals that describe the oscillatory contribution of a mode are probably similar, mathematically, for most systems. Some judgement as to the oscillatory contribution of a mode can then be made once the characteristic damping and oscillation frequencies of the mode are known.

REFERENCES

1. Stettner, R., Time-Dependent, Analytic, Electromagnetic Solution for a Highly Conducting Sphere, Mission Research Corporation, MRC-R-258, DNA 3910T, March 1976.

2. Stettner, R., A Non-Reflecting Electromagnetic Outer Boundary Condition for Cylindrical Coordinates and the SGEMP Problem, Mission Research Corporation, MRC-R-194, DNA 3890T, June 1975.

3. Gradshteyn, I. S., and I. W. Ryzhik, Tables of Integrals Series and Products, Academic Press, Inc., 1972.

4. Stratton, J. A., Electromagnetic Theory, McGraw-Hill Book Company, New York, 1941.

5. Stettner, R., and D. F. Higgins, X-ray Induced Currents on the Surface of a Metallic Sphere, Mission Research Corporation, MRC-N-111, DNA 3612T, April 16, 1975.

6. Lee, K.S.H., and L. Marin, "A Charged Particle Moving Near Perfectly Conducting Sphere," IEEE Trans. Antennas Propagat., Vol. AP-22, September 1974.